JPET Fast Forward. Published on September 15, 2017 as DOI: 10.1124/jpet.117.243451
This article has not been copyedited and formatted. The final version may differ from this version.

Hybrid of DNA-targeting Chlorambucil with Pt(IV) Species to Reverse Drug Resistance

Feihong Chen, Gang Xu, Xiaodong Qin, Xiufeng Jin, and Shaohua Gou

Jiangsu Province Hi-Tech Key Laboratory for Biomedical Research, Pharmaceutical Research Center and School of Chemistry and Chemical Engineering, Southeast University, Nanjing 211189, China

JPET Fast Forward. Published on September 15, 2017 as DOI: 10.1124/jpet.117.243451
This article has not been copyedited and formatted. The final version may differ from this version.

Running title: Pt(IV) species with chlorambucil to reverse drug resistance

Corresponding author: Shaohua Gou

Jiangsu Province Hi-Tech Key Laboratory for Biomedical Research, Pharmaceutical Research Center and School of Chemistry and Chemical Engineering, Southeast University, Nanjing 211189, China

E-mail: sgou@seu.edu.cn

Number of text pages: 46

Number of tables: 1

Number of figures: 9

Number of references: 53

Number of words in the abstract: 145

Number of words in the introduction: 785

Number of words in the discussion: 1010

ABBREVIATIONS: TBTU, O-(benzotriazol-1-yl)-N,N,N',N'-tetramethyluronium tetrafluoroborate; TEA, trimethylamine; DMF, N,N'-dimethylformamide; CDDP, cisplatin; DMSO, dimethylsulfoxide; PBS, phosphate buffer solution.

JPET Fast Forward. Published on September 15, 2017 as DOI: 10.1124/jpet.117.243451
This article has not been copyedited and formatted. The final version may differ from this version.

ABSTRACT

Two hybrids of Pt(IV) species were designed and prepared by addition of a chlorambucil unit to the axial positions of the Pt(IV) complexes derived from DN603 and DN604. *In vitro* studies of two hybrids against two pairs of cisplatin sensitive and resistant cancer cell lines indicated that compound **5** had superior antitumor activity to cisplatin and chlorambucil via suppressing DNA damage repair to reverse drug resistance. Mechanistic investigation suggested that the potent antitumor activity of compound **5** arose from its major suppression of CK2-mediated MRE11-RAD50-NBS1(MRN) complex promotion of DNA double-strand break (DSB) repair. In nude mice with A549/CDDP xenografts, compound **5** exhibited higher anticancer efficacy than cisplatin and chlorambucil via reversing drug resistance, displayed improved effectiveness and had hardly toxicity effects. Overall, compound **5** is a promising drug candidate, which could promote the anticancer activity and reverse drug resistance via attenuating CK2-induced MRN-dependent DSB repair.

Introduction

DNA-damaged agents are essential components of the most potent anticancer chemotherapeutics widely applied in clinic. Pt(II)-based chemotherapy drugs such as cisplatin, carboplatin and oxaliplatin have been proved to function via triggering persistent DNA damage to induce cell death (Rosenberg et al., 1969). The DNA damage induced by such DNA-targeted agents could be survived by specific DNA damage repair pathways, thus leading to innate and acquired resistances to limit the clinical applications of DNA-targeted agents (O'Grady et al., 2014; Cobo et al., 2007). It is also well known that severe side effects of cisplatin against gastrointestinal tract and kidneys have limited its wide usage (Klein and Hambley, 2009), which be mitigated via structural modification. Therefore, carboplatin was designed to decrease the adverse effects of cisplatin, which could be attributed to the inclusion of 1,1-cyclobutyldicaboxylate as the leaving group. As a result, the leaving ligand plays a significant role in determining the toxicity and side effects of a platinum drug. With the purpose of retaining the advantage of 1,1-cyclobutanedicarboxylate as a leaving ligand and also improving the kinetic properties of the resulting platinum complexes, we have introduced a carbonyl group to the skeleton of 1,1-cyclobutanedicarboxylate, in which the functionalized moiety (carbonyl group) could achieve the desired balance between hydrophilicity and lipophilicity of the resulting platinum complex and may improve the kinetic properties as well as the DNA-binding ability of the derivatives (Zhao et al., 2014). Such platinum complexes, named DN603 and DN604

JPET Fast Forward. Published on September 15, 2017 as DOI: 10.1124/jpet.117.243451
This article has not been copyedited and formatted. The final version may differ from this version.

(Fig. 1, upper panel), have been investigated, and subsequent researches demonstrated that DN604 could exhibit significant anticancer activity and reverse cisplatin resistance in cancer chemotherapeutics as well.

Chlorambucil, a member of the nitrogen mustard class of lipophilic DNA alkylating agents, is widely used for the treatment of human solid tumors (Chabner et al., 2011). Chlorambucil modifies DNA through the formation of either mono- or bifunctional adducts (Kohn, 1980). Mono-adducts interfere with gene expression and promote mismatched base-pairing, while bifunctional alkylation creates intra- and interstrand cross-links that inhibit DNA synthesis and induce DSBs (Kohn et al, 1987; Hemminki and Ludlum, 1983). Thus, exposure to chlorambucil leads to apoptotic cell death via the accumulation of extensive DNA damage (Hansson et al., 1987). The drug resistance and toxic effects associated with chlorambucil are serious impediments of therapeutic efficacy. In terms of drug resistance, sensitivity to chlorambucil is tempered by DSB repair mechanisms that are often up-regulated in common cancer tumors (Mao et al., 2009; Li et al., 2012).

DSBs are life-threatening lesions whose repair is promoted by an intricate network of multiple DNA repair pathways. The MRE11-RAD50-NBS1(MRN) complex is essential for repair of DSBs and stalled replication forks (Morgen et al., 2017). MRE11, NBS1 and RAD50 form the MRN complex that allows recognition of DSBs, activates two major DDR kinases ataxia-telangiectasia mutated (ATM) and ataxia-telangiectasia and Rad3 related (ATR), stabilizes ends of broken DNA and

JPET Fast Forward. Published on September 15, 2017 as DOI: 10.1124/jpet.117.243451
This article has not been copyedited and formatted. The final version may differ from this version.

facilitates DNA repair by homologous recombination (HR) and non-homologous end-joining (Williams et al., 2010; Cannavo and Cejka, 2014). Therefore, severe DNA damage repair-induced drug resistance could be destructed by the inhibitors of MRN-mediated DSB repair. Based on that, the approach of combing drugs with the inhibition of DSB repair in a molecule may have the potential superiority to reverse drug resistance.

The octahedral Pt(IV) complex with two additional coordination sites, exhibiting kinetic inertness and high accumulation in tumor tissues, is exploited for administration with few side effects, which have been considered to mitigate the limitations of corresponding Pt(II)-based drugs. As the first bifunctional Pt(IV) complex with two dichloroacetate (DCA) moieties in the axial positions, mitaplatin was found to attack nuclear DNA and mitochondria to heighten cancer cell apoptosis (Dhar et al., 2011). Moreover, Platin-A, a hybrid of Pt(IV)-aspirin, was designed to release aspirin, which exhibited anticancer and anti-inflammatory features better than the monotherapy (Fig.1, lower panel) (Pathak et al., 2014). Although the known Pt(IV) complexes shown superior ability to reverse platinum resistance via other possible mechanisms (Chen et al., 2017), specific DSB repair pathways that play an important role in the platinum resistance response have not been studied. Hence, multi-targeted Pt(IV) hybrids which could suppress DSB repair response are most promising to overcome the resistance of some Pt(II) drugs. Due to the multiple biological functions of chlorambucil, it is rational to design hybrid compounds by conjugating a

chlorambucil unit into a Pt(IV) complex so as to introduce the anticancer activity of chlorambucil and reduce the toxicity of Pt(II) complexes. In this paper, two novel Pt(IV) hybrids containing a chlorambucil unit in the axial position were investigated for their effects on cisplatin resistant cancer cells via inhibiting DSBs response-mediated pathway. In our assumption, the new compounds could not only show enhanced antitumor property, but also exhibit the resistance prevention via acting on multiple targets.

Materials and methods

Materials and general measurements. Common chemicals and solvents were purchased from Sinopharm Chemical Reagent Co. DN604 (**1**) and DN603 (**2**) were prepared as described previously (Zhao et al., 2014). Elemental analyses for C, H, and N were done on a Vario MICRO CHNOS Elemental Analyzer (Elementar). ^{1}H and ^{13}C spectra of the corresponding platinum(IV) complexes were measured in d_6-DMSO with a Bruker 300 MHz spectrometer and chemical shifts were internally referenced to solvent signals. Electrospray ionization mass spectrometry (ESI-MS) was measured on an Agilent 6224 TOF LC/MS instrument. Fluorescence spectra were recorded on a Hitachi F-4600 fluorescence spectrometer using a 1 cm path length cuvette. Inductively coupled plasma-optical emission spectrometer (Optima 2100DV, PE, USA) was determined to detect platinum contents. Distilled water was purified by passage through a Millipore Milli-Q Biocel water purification system (18.2 MV)

JPET Fast Forward. Published on September 15, 2017 as DOI: 10.1124/jpet.117.243451
This article has not been copyedited and formatted. The final version may differ from this version.

equipped with a 0.22 μm filter. 96-well plate reader analyses were performed on a Thermo's microplate absorbance reader. Flow cytometry studies were performed on a BD LSRII flow cytometer equipped with Cell-Quest software from BD Biosciences. Confocal images were recorded in an Olympus FV1000 confocal microscope.

Procedure for synthesis of 3. N-chlorosuccinimide (29.38 mg, 0.22 mmol) dissolved in 14 mL of water was added to a suspension of **1** (84.75 mg, 0.22 mmol) in 6 mL of water. The reaction was stirred at room temperature for 3 h in the dark. The solid residue was removed by centrifugation and the solution was evaporated to dryness to get a pale yellow solid that was washed with ethanol and diethylether. Yield: 78.96 mg (82%). ^{1}H NMR (300 MHz, DMSO-d_6): δ 2.95 (s, 1H), 3.45 (s, 2H), 3.49 (s, 2H), 5.90-5.72 (m, 6H) ppm. ^{13}C NMR (75 MHz, DMSO-d_6): δ 45.62, 59.67, 60.21, 176.37, 204.40 ppm.

Procedure for synthesis of 4. N-chlorosuccinimide (29.38 mg, 0.22 mmol) dissolved in 14 mL of water was added to a suspension of **2** (102.38 mg, 0.22 mmol) in 6 mL of water. The reaction was stirred at room temperature for 3 h in the dark. The solid residue was removed by centrifugation and the solution was evaporated to dryness to get a pale yellow solid that was washed with ethanol and diethylether. Yield: 96.83 mg (85%). ^{1}H NMR (300 MHz, DMSO-d_6): δ 1.00-1.12 (m, 2H), 1.41 (dd, J = 22.4, 11.2 Hz, 1H), 1.47(d, J = 7.9 Hz, 3H), 1.96 (d, J

= 10.6 Hz, 1H), 2.02 (d, J = 11.2 Hz, 1H), 2.59 (dd, J = 22.3, 11.8 Hz, 2H), 2.82 (s, 1 H), 3.43 (d, J = 5.3 Hz, 2H), 3.48 (d, J = 5.1 Hz, 2H), 7.04 (t, J = 9.5 Hz, 1H), 7.18 (t, J = 9.4 Hz, 1H), 7.58 (d, J = 6.3 Hz, 1H), 7.86 (d, J = 6.8 Hz, 1H) ppm. ^{13}C NMR (75 MHz, DMSO-d_6): δ 23.69, 23.84, 30.35, 30.80, 45.68, 59.97, 60.07, 60.99, 61.77, 176.45, 176.55, 204.30 ppm.

Procedure for synthesis of 5. A solution of TBTU (96.33 mg, 0.30 mmol) and chlorambucil (60.84 mg, 0.20 mmol) in 10 mL of DMF dry was stirred at room temperature under N_2 atmosphere. After 10 min, TEA (41.73 μL, 0.30 mmol) was added and reaction was stirred for 15 min. **3** (87.54 mg, 0.20 mmol) was then added and the reaction mixture was stirred at room temperature for 12 h. The solvent was then removed by evaporation under reduced pressure. The product was isolated by direct-phase chromatography using silica as stationary phase and a solution of 15:1 dichloromethane/methanol as eluent. Yield: 65.15 mg (45%). ESI-MS: *m/z* $[M-H]^-$ = 722.05. ^{1}H NMR (300 MHz, DMSO-d_6): δ 1.67-1.72 (2H, m), 2.21-2.26 (2H, m), 2.42-2.45 (2H, m), 3.49 (4H, s), 3.68 (8H, s), 6.28 (6H, m), 6.63-6.66 (2H, d), 6.99-7.02(2H, d) ppm. ^{13}C NMR (75 MHz, DMSO-d_6): δ 28.02, 33.91, 35.34, 41.66, 46.22, 52.72, 60.02, 60.16, 112.32, 129.92, 130.51, 144.86, 176.29, 176.42, 179.43, 204.15 ppm. Anal. Calcd (%) for $C_{20}H_{28}Cl_3N_3O_7Pt$: C 33.18, H 3.90, N 5.80. Found: C 32.89, H 4.15, N 5.57.

JPET Fast Forward. Published on September 15, 2017 as DOI: 10.1124/jpet.117.243451
This article has not been copyedited and formatted. The final version may differ from this version.

Procedure for synthesis of 6. A solution of TBTU (96.33 mg, 0.30 mmol) and chlorambucil (60.84 mg, 0.20 mmol) in 10 mL of DMF dry was stirred at room temperature under N_2 atmosphere. After 10 min, TEA (41.73 μL, 0.30 mmol) was added and reaction was stirred for 15 min. **4** (87.54 mg, 0.20 mmol) was then added and the reaction mixture was stirred at room temperature for 12 h. The solvent was then removed by evaporation under reduced pressure. The product was isolated by direct-phase chromatography using silica as stationary phase and a solution of 15:1 dichloromethane/methanol as eluent. Yield: 77.18 mg (48%). ESI-MS: *m/z* $[M-H]^-$ = 802.12. ^{1}H NMR (300 MHz, DMSO-d_6): δ 1.07-1.51 (6H, m), 1.70-1.74 (2H, m), 1.98-2.11 (2H, m), 2.25-2.30 (2H, m), 2.42-2.45 (2H, m), 2.56-2.68 (2H, m), 3.38 (2H, s), 3.52 (2H, s), 3.69 (8H, s), 6.63-6.65 (2H, d), 6.99-7.02 (2H, d), 7.97-8.55 (4H, m) ppm. ^{13}C NMR (75 MHz, DMSO-d_6): δ 23.94, 24.04, 27.08, 30.98, 31.37, 33.82, 36.41, 41.65, 46.29, 52.72, 59.12, 60.70, 61.99, 62.21, 112.36, 129.83, 130.35, 144.90, 176.51, 176.59, 180.55, 203.94 ppm. Anal. Calcd (%) for $C_{26}H_{36}Cl_3N_3O_7Pt$: C 38.84, H 4.51, N 5.23. Found: C 38.65, H 4.60, N 4.99.

Cell culture. Cisplatin-sensitive SGC-7901 and A549 cancer cell lines, and cisplatin-resistant SGC-7901/CDDP and A549/CDDP cancer lines as well as normal HUVEC cell line were purchased from the Cell Bank of Shanghai Institute of Cell Biology. HUVEC cells were cultured at 37 ℃ in 5% CO_2 with DMEM supplemented with 10% fetal bovine serum (FBS) (Hyclone, Lifescience, USA), 100

JPET Fast Forward. Published on September 15, 2017 as DOI: 10.1124/jpet.117.243451
This article has not been copyedited and formatted. The final version may differ from this version.

U/mL benzyl penicillin and 100 mg/mL streptomycin (Beyotime, Nantong, China), while SGC-7901 and A549 cancer cells were cultured at 37 ℃ in 5% CO_2 with RPMI-1640 supplemented with 10% FBS and 100 U/mL benzyl penicillin and 100 mg/mL streptomycin. Moreover, SGC-7901/CDDP and A549/CDDP cancer cells were cultured and screened in RPMI-1640 supplemented with 10% FBS, 100 U/mL benzyl penicillin, 100 mg/mL streptomycin and 800 ng/mL cisplatin before use. Cells were passed every 2 days and restarted from frozen stocks upon reaching pass number 20.

***In vitro* cell viability assay.** Cytotoxicity profiles of the tested compounds against different cell lines were evaluated by the MTT assay. Cells were plated at density of 10^5/mL per well in 96-well plates. After overnight growth, cells were exposed to medium containing the tested compounds separately at varying concentrations and incubated for 72 h at 37 ℃. Then the cell viability was determined by the MTT method according to previous description (Chen et al., 2012).

Reactions of compound 5 with DNA. Herring sperm DNA was dissolved in 10 mM phosphate buffer (pH 7.4) containing 10 mM $NaClO_4$. The DNA concentration was determined by UV-vis spectra at 260 nm with an extinction coefficient of 6600 M^{-1}. The mixture of DNA with platinum compounds were incubated at 37 ℃ in the dark. The fluorescence was measured in 0.4 M NaCl to avoid the second fixation site

JPET Fast Forward. Published on September 15, 2017 as DOI: 10.1124/jpet.117.243451
This article has not been copyedited and formatted. The final version may differ from this version.

of EtBr to DNA. EtBr (0.04 mg/mL) was added to the 0.01 mg/mL DNA solution before the fluorescence measurement. Ascorbic acid was added for the reduction of compound **5**. Fluorescence spectra were recorded under following conditions: scan speed 2000 nm min^{-1}; excitation slit width was 5 nm and emission slit width was 10 nm. The excitation and emission wavelength was 530 nm and 592 nm, respectively.

Cellular platinum uptake and DNA platination assay. The cellular uptakes of cisplatin, compound **5** were measured on A549 and A549/CDDP cells. The cells were seeded in 6-well plates overnight and then incubated with 15 μM cisplatin and compound **5** at 37 °C (unobstructed interaction) or at 4 °C (interaction partially inhibited) in standard culture conditions. After 4 h, the cells were washed with PBS buffer (pH 7.4) for three times, and harvested by trypsinization. After re-suspension in PBS, the pellet was washed with PBS and collected per centrifugation (5910R, Eppendorf) at 500 g for 5 min at 4 ℃. The organelles were then isolated via differential centrifugation. All cellular compartments (mitochondria, lysosomes and nucleus) were isolated from A549 and A549/CDDP cells for direct comparative purposes. The supernatant phases discarded during the isolation of nuclei, lysosomes and mitochondria procedures were collected and formed the “residual” fraction. An aliquot of crude lysate after homogenization, nuclear, mitochondrial (pellet lysedvia freeze and thaw cycles followed by 20 min incubation in ultrasonic bath), lysosomal and residual fraction was each used for protein quantification using the Bradford

JPET Fast Forward. Published on September 15, 2017 as DOI: 10.1124/jpet.117.243451
This article has not been copyedited and formatted. The final version may differ from this version.

method (Siddiqui-Jain et al., 2010). The harvested cells were concentrated and digested by nitric acid for the ICP measurement. The cell numbers were counted before the digested. For the measurement of Pt concentration in cellular DNA in A549 and A549/CDDP cells, DNA was isolated by applying Genomic DNA Mini Preparation Kit (Beyotime, China), and Pt content in DNA was analyzed by ICP.

Apoptosis assessment. The apoptosis induced by compound **5** was detected by Annexin V-FITC apoptosis detection kit according to the manufacturer's protocol. Briefly, cells were treated with 15 μM chlorambucil, cisplatin, DN604 and compound **5**, respectively for 24 h at 37 ℃. Then the cells were collected, resuspended in binding buffer (pH 7.5, 10 mM HEPES, 2.5 mM $CaCl_2$ and 140 mM NaCl), and incubated with Annexin V-FITC and then PI for 10 min in the dark at room temperature, cells were analyzed by flow cytometry (FACSCalibur, Becton Dickinson, USA) and a computer station running Cell-Quest software (BD Biosciences, Franklin Lakes, NJ, USA).

Analysis of caspase-3 activation. For the quantification of activation of caspase-3 in cancer cells, 5×10^5 cancer cells were seeded in a 60 mm dish and allowed to adhere for 1 day. The cells were incubated with cisplatin, DN604 and compound **5** at a concentration of 15 μM for 24 h to induce the activation of caspase-3. As a reference control, the cells were only incubated with fresh media at 37 ℃. Then, the cells were

JPET Fast Forward. Published on September 15, 2017 as DOI: 10.1124/jpet.117.243451
This article has not been copyedited and formatted. The final version may differ from this version.

washed with PBS to eliminate the remaining drugs and harvested using trypsin-EDTA. All the groups of cells were collected into microtubes following incubation with 300 mL media containing 1 mL of FITC-DEVD-FMK (Caspase 3(active) FITC Staining Kit (ab65613)) for 1 h at 37 ℃ under 5% CO_2. Subsequently, centrifugation of the cells was performed to collect cell pellets and washed 2 times with washing buffer. Each group of cells was resuspended with 300 mL of the washing buffer and transferred 100 mL per well in a microtiter plate reader. The quantification of caspase-3 was evaluated as Relative Fluorescence Unit (RFU) using Fluorophotometer (Max Gemini EM, SoftMax® Pro 5, Molecular Devices Corp., Sunnyvale, CA) at an emission wavelength of 535 nm after excitation at 485 nm. The statistical significance was evaluated with one-way ANOVA test using Graph Pad Prism 4 software.

Colony formation assay. Cells were trypsinized and plated at a density of 500 perplate. Fourteen days later, 15 μM chlorambucil, cisplatin, DN604 and compound **5** in cell culture medium were added to the plates, and cells were incubated for a further 7 days. Cells were then fixed with 3% paraformaldehyde, stained with crystal violet and imaged with a light microscope. The experiment was performed in triplicate. The number of colonies, defined as containing > 50 cells, was counted.

JPET Fast Forward. Published on September 15, 2017 as DOI: 10.1124/jpet.117.243451
This article has not been copyedited and formatted. The final version may differ from this version.

Cell-cycle analysis. Cell cycle was analyzed by flow cytometry as described previously (Chen et al., 2010). Data were analyzed with FlowJo software (TreeStar, Inc.).

Analysis of intracellular K^+ leakage. A549 and A549/CDDP cancer cells were incubated with 15 μM chlorambucil, cisplatin, DN604 and compound **5** at 37 ℃ for 4 h. After every 1 h interval during incubation, the suspensions were collected, and supernatants were trans-ported. Extracellular K^+ concentration was measured using anion selective electrode meter (Orion Star A214, Thermo Scientific, Singapore). The K^+ concentration was calculated using the following formula: K^+ leakage (%) = $([K^+]-[K^+]_0)/([K^+]_t-[K^+]_0) \times 100$, where $[K^+]$ is the K^+ leakage induced by each compound, and $[K^+]_0$ and $[K^+]_t$ are the K^+ leakage without the compounds and with sonication, respectively. Here, sonicated cells (1 min, 60 amplitude) were used to determine 100% K^+ leakage (Yannopoulos et al., 2015; Arduino et al., 2009).

Analysis of cytosolic and mitochondrial Ca^{2+} levels. A549 and A549/CDDP cancer cells were incubated with 15 μM chlorambucil, cisplatin, DN604 and compound **5** at 37 ℃ for 4 h. After incubation, the cells were washed three times with Krebs buffer (132 mM NaCl, 4 mM KCl, 1.4 mM $MgCl_2$, 6 mM glucose, 10 mM HEPES, 10 mM $NaHCO_3$, and 1 mM $CaCl_2$, pH 7.2), with 0.01% Pluronic F-127 (Molecular Probes, Eugene, OR, USA) and 1% bovine serum albumin were added to

the cells. The suspensions were incubated with Rhod-2AM (10 μM) or Fura-2AM (5 μM) (Molecular Probes, Eugene, OR, USA) at 37 ℃ for 30 min, then washed three times with calcium-free Krebs buffer. The fluorescence intensities of Fura-2AM (excitation-335 nm, emission-505 nm) and Rhod-2AM (excitation-550 nm, emission-580 nm) were analyzed using a spectrofluorophotometer (Shimadzu RF-5301PC, Shimadzu, Kyoto, Japan) (Valipour et al., 2015; Alonso-Monge et al., 2009).

Mitochondrial transmembrane potential (ΔΨm) assessment. The electrical potential difference across inner mitochondrial membrane (ΔΨm) was monitored using the ΔΨm-specific fluorescent probe JC-1 (Molecular Probes Inc., Eugene, OR), a sensitive fluorescent dye. Briefly, the cancer cells treated with 15μM of cisplatin, chlorambucil, DN604 or compound **5** for 24 h were harvested with ice-cold PBS and resuspended in RPMI-1640 medium at a density of 0.5×10^6 cells/ml, then the cells were permeabilized with 0.3% Triton X-100, washed with ice-cold PBS, incubated with 10 μM JC-1 for 15 min at 37 ℃ in the dark and observed under a fluorescence microscope (Olympus IX51, Japan). Red fluorescence is attributable to a potential-dependent aggregation in the mitochondria. Green fluorescence, reflecting the monomeric form of JC-1, appeared in the cytosol after mitochondrial membrane depolarization. Relative fluorescence intensities were monitored using the flow cytometry (FACSCalibur, Becton Dickinson), and analyzed by the software Modfit

and Cell Quest (BD Biosciences, Franklin Lakes, NJ) with settings of FL1 (green) at 530 nm and FL2 (red) at 585 nm.

Measurement of ATP production. The ATP production assay kit (Haimen, Jiangsu, China) was used to measure intracellular ATP level according to the manufacturer's instructions. In brief, cells were treated with 15μM of chlorambucil, cisplatin, DN604 and compound **5**, respectively, for 12 h, then incubated with 100 μL Nuclear Releasing Reagent for 5 min at 37 ℃ with gentle shaking, followed by further incubation with 1 μL ATP monitoring enzyme. Detection was performed using the luminometer Orion II (Berthold DS, Bleichstr, Pforzheim, Germany).

ROS measurement. The generation of ROS induced by compound **5** was determined with the cell permeant fluorogenic probe 2',7'-dichlorodihydrofluorescein diacetate (H_2DCFDA; Molecular Probes, Invitrogen, Darmstadt, Germany). H_2DCFDA diffuses into the cell, where it is enzymatically converted by intracellular esterases and oxidized into the high fluorescence compound DCF, which allows the determination of H_2O_2, peroxynitrite anions and peroxyl radicals. Approximately 4×10^3 A549 and A549/CDDP cells per well were plated on white bottom 96-well plates in extracellular fluid (140 nM NaCl, 3 mM KCl, 1 mM $CaCl_2$, 1 mM $MgCl_2$, 10 mM HEPES and 25 mM glucose; pH 7.4). After 24 h incubation, cells were treated with 15 μM chlorambucil, cisplatin, DN604 and compound **5** for 6 h at 37 ℃. Then,

JPET Fast Forward. Published on September 15, 2017 as DOI: 10.1124/jpet.117.243451
This article has not been copyedited and formatted. The final version may differ from this version.

cells were loaded with 10 mM H_2DCFDA for 30 min at 37 ℃ and 5% CO_2. Then, cells DCF generation was measured over time using a fluorometer (Fluostar BMG Labtech, Offenburg, Germany) at 492 nm excitation and 520 nm emission.

H_2O_2 measurement. The production of H_2O_2 was determined with the Amplex® Red reagent (10-acetyl-3,7-dihydroxyphenoxazine; Molecular Probes). In the presence of horse radish peroxidase (HPR), the Amplex® Red reagent reacts in a 1:1 stoichiometry to produce the red-fluorescent oxidation product, resorufin. Consequently, resorufin generation allows the detection of the H_2O_2 released from biological compounds. Approximately 4×10^3 A549 and A549/CDDP cancer cells were plated on black bottom 96-well plates in 120 ml of working solution containing 40 mM Amplex® Red reagent and 0.1 U/ml HPR, and incubated in the presence of 15 μM chlorambucil, cisplatin, DN604 and compound **5** for 2 h at 37 ℃. Resorufin generation was measured over time using a fluorometer (Fluostar BMG Labtech) at 544 nm excitation and 590 nm emission.

Intracellular GSH measurement. A549 and A549/CDDP cancer cells in 6 cm culture plates were treated as follows: 15 μM chlorambucil, cisplatin, DN604 and compound **5**. After 4 h, medium was removed and dishes were rinsed three times with cold PBS. The cells were harvested and cell numbers were counted. Then,

JPET Fast Forward. Published on September 15, 2017 as DOI: 10.1124/jpet.117.243451
This article has not been copyedited and formatted. The final version may differ from this version.

intracellular GSH levels were measured using a GSH test kit (KeyGen KGT006). A549 and A549/CDDP cancer cells without treatment were used as control groups.

Comet assay. A549 and A549/CDDP cells (1×10^5 cells) treated with 15 μM chlorambucil, cisplatin, DN604 and compound **5** for 24 h were combined with molten LM Agarose (Trevigen) at a ratio of 1:10 (v/v) and were immediately pipetted onto Comet Slide (Trevigen). Slides were incubated at 4 ℃ in the dark for 10 min, then immersed in prechilled Lysis buffer and incubated at 4 ℃ for 30 min. Slides were immersed in alkaline unwinding solution, pH > 13 (200 mM NaOH, 1 mM EDTA) for 20 min at room temperature in the dark. Electrophoresis was done at 21 V for 30 min using alkaline electrophoresis solution (200 mM NaOH, 1 mM EDTA). The slides were washed twice in water for 5 min and once in 70% EtOH for 5 min, then dried overnight and visualized by microscopy. The cells were analyzed by Comet Assay Software Project (CASP).

Determination of DNA lesion frequency by quantitative PCR. Determination of DNA lesion frequency was determined from a published method (Fonseca et al., 2011). A total of 1×10^6 A549 and A549/CDDP cancer cells were treated with cisplatin and compound **5** (15 μM) for 4 h. Then DNA was isolated from frozen cell pellets using the QIAGEN Genomic Tip and quantified via PicoGreen dye (Invitrogen). Quantitative amplification of the 8.9 kb mitochondrial segment and the 17.7 kb

JPET Fast Forward. Published on September 15, 2017 as DOI: 10.1124/jpet.117.243451
This article has not been copyedited and formatted. The final version may differ from this version.

b-globin target sequence was performed using the GeneAmp XL PCR kit (Perkin-Elmer). Lesion frequency at a given dose, D, was calculated as $D = -\ln A_D/A_C$, where A_D is the amplification at the dose, and A_C is the level of amplification in untreated controls.

Immunofluorescence and foci detection. Briefly, A549 and A549/CDDP cells were grown to confluence in 35 mm sterile dishes with 0.17 mm glass bottom for 24 h at 37 ℃. After treatment of 15 μM chlorambucil, cisplatin, DN604 and compound **5**, respectively, for 24h, cells were washed with PBS, fixed in 4% paraformaladehyde/PBS for 0.5 h and permeabilized with PT-5 solution [0.3% Triton X-100 in PBS] for 30 min at 4 ℃. The cells were blocked by incubating with PTB-5 [0.5% BSA in PBS] for 1 h at R.T. Dishes were then incubated with primary antibody (1:500) overnight at 4 ℃. Cells were stained with secondary antibody conjugated with Alexa 488 (1:100, Invitrogen, Carlsbad, USA) and the DNA counterstained with 1 mM DAPI (Invitrogen, USA). Microscopy was performed on a Leica TCS NT confocal scanner equipped with an ArKr-Laser on the Leica DM IRBE inverted microscope (lens: HCX PlanApo 63x oil/NA1.32). Confocal images were displayed as maximum projections and assembled in Adobe Photoshop 7.0. Slides for the foci detection were produced and counted in 120 cells per slide. The results could be recorded as both foci values per cell and the percentage of cells with 4 or ≥ 10 foci.

JPET Fast Forward. Published on September 15, 2017 as DOI: 10.1124/jpet.117.243451
This article has not been copyedited and formatted. The final version may differ from this version.

Western blot analysis. After the treatment of the indicated concentration of 15 μM cisplatin, DN604 and compound **5** for 24 h, A549 and A549/CDDP cells were collected and lysed in lysis buffer (100 mM Tris-Cl, pH 6.8, 4% (m/v) sodium dodecylsulfonate, 20% (v/v) glycerol, 200 mM β-mercaptoethanol, 1 mM phenylmethylsulfonyl fluoride, and 1 g/ml aprotinin). Lysates were centrifuged at 12,000 g for 0.5 h at 4°C. The concentrations of total proteins were measured using the BCA assay method with Varioskan spectrofluorometer and spectrophotometer (Thermo, Waltham, MA) at 562 nm. Protein (20-100 μg) prepared from the indicated cells was loaded per lane and electrophoresed in 8% or 10% sodium dodecyl sulfate polyacrylamide gel electrophoresis (SDS-PAGE), and then transferred onto polyvinylidene difluoride (PVDF) Immobilon-P membrane (Bio-Rad, USA) using a transblot apparatus (Bio-Rad, USA). The membranes were blocked with 5% (w/v) non-fat milk at 0.5 h at 37 ℃, followed by overnight incubation at 4 ℃ with primary antibodies diluted in PBST. After washing with PBST, the membranes were incubated for 1 h with an IRDye × 800 conjugated secondary antibody diluted 1:20000 in PBST, and the labeled proteins were detected with an Odyssey Scanning System (Li-COR., Lincoln, Nebraska, USA).

CK2 activity assay. The CK2 activity was detected with the CK2 assay kit treated with 15 μM cisplatin, DN604 and compound **5,** respectively, according to manufacturer's instruction (Chen et al., 2012).

JPET Fast Forward. Published on September 15, 2017 as DOI: 10.1124/jpet.117.243451
This article has not been copyedited and formatted. The final version may differ from this version.

***In vivo* antitumor efficacy of compound 5.** Thirty-five nude mice (BALB/c) with body weight range from 18-22 g, were supplied by Shanghai Laboratory Animal Center, China Academy of Sciences. Experimental protocols were in accordance with National Institutes of Health regulations and approved by the Institutional Animal Care and Use Committee. All animals were randomly divided into 5 groups. The cisplatin resistant A549/CDDP single-cell suspension in PBS (1×10^7 cells per mouse) was injected subcutaneously into the right oxter of nude mice. When tumor grew to a size of 80-150 mm^3 at 12 days, the mice were administrated via cisplatin (dosed intravenously at 5 mg/kg twice a week), chlorambucil (dosed intravenously at 5 mg/kg once every three days), DN604 (dosed intravenously at 5 mg/kg once every three days), compound **5** (dosed intravenously at 5 mg/kg once every three days). The control group was administered glucose. The tumor growth was monitored by measuring the perpendicular diameter of the tumor using calipers every two days and calculated according to the formula:

$$\text{Tumor volume } (mm^3) = 0.5 \times \text{length} \times \text{width}^2$$

Growth curves were plotted using the average tumor volume within each experimental group at the set time points. The whole group of mice was sacrificed after the last treatment, then tumor weight was evaluated as the antitumor activity of the corresponding groups, and the kidneys, livers and tumors were excised for

JPET Fast Forward. Published on September 15, 2017 as DOI: 10.1124/jpet.117.243451
This article has not been copyedited and formatted. The final version may differ from this version.

immunohistochemistry analysis. The body weight and physical state of the mice were measured simultaneously as an indicator of systemic toxicity.

Blood stability test of compound 5 with rat plasma. To a volume of 0.6 mL rat plasma was added 10 μL of a DMSO solution of compound **5** (10 mM), resulting in a final concentration of 50 μM. At varying time points (0, 2, 4 and 8 h) at 37 ℃, a 300 μL aliquot was removed from the incubating blood. The ICP-MS measurement was served to confirm the blood stability of compound **5** in rat plasma.

Pharmacokinetics studies. Twenty-four SD rats (240-250 g) were supplied by Shanghai Laboratory Animal Center, China Academy of Sciences. Experimental protocols were in accordance with National Institutes of Health regulations and approved by the Institutional Animal Care and Use Committee. SD rats composed of half male and half female were randomly divided into 2 groups: 1) cisplatin (5 mg/kg); 2) compound **5** (5 mg/kg). 0.6 ml of blood samples were collected from orbital cavity at 5 min followed by 0.5, 1, 2, 4, 8, 12 and 24 h after intravenous administration, heparinized and then centrifuged at 4000 rpm for 20 min at 4 ℃. The supernatant plasma was collected for measurement of Pt content using ICP-MS. The apparent plasma half-life time was calculated using a Phoenix Win Nonlin 6.3 Program (Pharsight Cooperation, St. Louis Missouri, USA).

JPET Fast Forward. Published on September 15, 2017 as DOI: 10.1124/jpet.117.243451
This article has not been copyedited and formatted. The final version may differ from this version.

Statistical analysis. The data shown in the study were expressed as means ± SD from at least 3 independent experiments, each in triplicate compounds for individual treatment or dosage. Statistical analyses were performed using an unpaired, two-tailed Student's t-test. All comparisons are made relative to untreated controls and significance of difference is indicated as $*P < 0.05$ and $**P < 0.01$.

Results

Design and synthesis. The synthetic route to prepare compounds **5** and **6** is depicted in Scheme 1. Chlorambucil was obtained according to a literature procedure (Fousteris et al., 2006). Meanwhile, Pt(IV) complexes **3** and **4** were synthesized through the oxidative chlorination of the corresponding Pt(II) complexes (**1** or **2**) with N-chlorosuccinimide (NCS) in water (Huang et al., 2016). Finally, compounds **5** and **6** were obtained via chlorambucil coupling with the corresponding Pt(IV) intermediate in the presence of O-(benzotriazol-1-yl)-N,N,N',N'-tetramethyluronium tetrafluoroborate (TBTU) as the coupling agent. The products were purified by column chromatography, and their structures were characterized by ^{1}H and ^{13}C NMR spectra together with ESI-MS spectrometer (Figs. 2 and 3).

Cytotoxicity effects. The *in vitro* cytotoxicity of compounds **5** and **6** together with their Pt(II) parent complexes, DN604 and DN603, was ascertained using MTT assays on a panel of human cancer cells including SGC-7901 (cisplatin-sensitive gastric cancer) and SGC-7901/CDDP (cisplatin-resistant gastric cancer), A549 (cisplatin-sensitive lung cancer) and A549/CDDP (cisplatin-resistant lung cancer) as well as human normal cell line HUVEC. Cisplatin, oxaliplatin, carboplatin and chlorambucil were used as the positive controls. As listed in Table 1, DN604 exhibited stronger cytotoxicity than cisplatin, carboplatin and oxaliplatin towards cisplatin-resistant SGC-7901/CDDP and A549/CDDP cancer cells. The results shown

that compound **5** exhibited 1.75-fold and 2.06-fold lower IC_{50} values towards SGC-7901/CDDP and A549/CDDP cancer cells than DN604, respectively, while 34.93-fold and 62.04-fold lower than chlorambucil. However, the IC_{50} value of compound **5** against SGC-7901 and A549 cancer cells was close to cisplatin, and those of compound **6** against all cancer cell lines were close to oxaliplatin and DN603. Notably, compound **5** exhibited a greater cytotoxic activity than its parent compounds in the test of cisplatin-resistant cancer cells. Such results proved that compound **5** has the potential to reverse cisplatin resistance of SGC-7901/CDDP and A549/CDDP cancer cells via reducing the drug resistant factor (RF) from 7.09 (cisplatin) to 0.81 and 9.59 (cisplatin) to 0.58, respectively. Besides, it is of much significance to note that both compounds **5** and **6** were less cytotoxic toward human normal HUVEC cells than DN603 and DN604. Similar results were shown in the dose-dependent curves of the tested cancer cells to cisplatin, DN604 and compound **5** using MTT assays (Fig. 5A, left panel). As compound **5** surpassed the antitumor activity of cisplatin and chlorambucil, it might act on an extra target different from that of traditional platinum-based compounds. Therefore, compound **5** was chosen for further study.

DNA platination induced via reduction. The cytotoxicity effect of compound **5** owing to the DNA platination could be determined in the presence of EtBr as a probe, for the DNA platination of Pt could be reduced via the formation of EtBr-DNA complex. The results in Fig. 4A showed that compound **5** did not induce much

fluorescent intensity change before it was reduced to a Pt(II) moiety in the presence of ascorbic acid (AsA), while cisplatin could definitely lead to the loss of fluorescent intensity. The results indicated that under the activation of reductant AsA, compound **5** can actually exert its cytotoxic effect.

Cellular uptake. In order to explore the mechanism of the improved cytotoxicity effect of compound **5** compared with cisplatin and DN604, the cellular uptake of cisplatin, DN604 and compound **5** was detected in cisplatin sensitive and cisplatin resistant cancer cells. After the treatment for 4 h, the platinum content in these cancer cells was analyzed via ICP technique. As results shown in Fig. 4B upper panel, the elevated cellular uptakes of compound **5** in cisplatin-resistant SGC-7901/CDDP and A549/CDDP cancer cells were dramatically 2.53-fold and 3.31-fold, respectively, higher than that of cisplatin, while in cisplatin-sensitive SGC-7901 and A549 cancer cells, 1.28-fold and 1.23-fold, respectively, lower than that of cisplatin. Notably, the platinum amount of compound **5** in HUVEC normal cells was 2.6-fold lower than that of cisplatin. The results of the Pt accumulation assays repeated at 4 ℃ showed that the incubation of cisplatin sensitive and resistant cells at low temperature led to a reduction in the Pt accumulation, which indicates that compound **5** enters the cells through an energy-dependent pathway and not exclusively by passive diffusion (Fig. 4B, lower panel).

Moreover, the amount of platinum in the different subcellular compartments of

JPET Fast Forward. Published on September 15, 2017 as DOI: 10.1124/jpet.117.243451
This article has not been copyedited and formatted. The final version may differ from this version.

cancer cells was quantified to fetch a more detailed picture of the intracellular localization of platinum complexes (Fig. 4C). As expected for cisplatin, which is known to induce cell death by forming adducts on nucleus DNA, 69% and 72% of the total intracellular Pt was located in the nucleus of cisplatin-sensitive SGC-7901 and A549 cancer cells, while only 21% and 29% in cisplatin-resistant SGC-7901/CDDP and A549/CDDP cancer cells. In contrast, the ratio was 69% and 72% for compound **5** in SGC-7901/CDDP and A549/CDDP cancer cells, respectively. These results bode well for a role of compound **5** to effectively bind to genomic DNA and overcome platinum resistance in SGC-7901/CDDP and A549/CDDP cancer cells.

Platinum-based drugs enter the cells by passive diffusion and through carrier-mediated uptake by a number of transport proteins in which several proteins have been identified as possible uptake transporters for platinating compounds (Hall et al., 2008). For copper transporter 1 (Ctr1), which controls intracellular copper homeostasis, an involvement in uptake of cisplatin has been shown (Ishida et al., 2002; Kuo et al., 2007). Thus the levels of Ctr1 protein in our tests were measured by immunoblotting. The results indicated that the amount of Ctr1 was reduced in cisplatin-resistant cancer cells compared to cisplatin-sensitive cancer cells, suggesting that reduced expression of Ctr1 contributed to the observed low levels of cisplatin in SGC-7901/CDDP and A549/CDDP cancer cells (Fig. 4D). It is discussed that chelator-mediated copper starvation leads to a conformational change of Ctr1 allowing more cisplatin to be transported into the cells resulting in the observed

JPET Fast Forward. Published on September 15, 2017 as DOI: 10.1124/jpet.117.243451
This article has not been copyedited and formatted. The final version may differ from this version.

increased platinum levels. When SGC-7901 and A549 cancer cells were pre-treated with TM for 24 h and then incubated with cisplatin for 2 h, we observed an up to 1.3-fold and 1.2-fold increase in intracellular platinum accumulation compared to cells incubated with cisplatin alone (Fig. 4E, upper panel). In contrast, intracellular platinum accumulation after incubation with compound **5** was not affected by TM in cisplatin-sensitive SGC-7901 and A549 cancer cells. As Ctr1 is expressed at low levels in cisplatin-resistant SGC-7901/CDDP and A549/CDDP cancer cells, manipulation of only few transporters might not exert a major influence on cisplatin uptake. Altogether these data support the hypothesis that compound **5** is mainly taken up by passive diffusion, while active transport mechanisms by Ctr1 seem to play a minor role. As a consequence, a change in active uptake mediated by transport proteins, observed in cisplatin-resistant SGC-7901/CDDP and A549/CDDP cancer cells, would not affect the influx of compound **5** (Fig. 4E, lower panel). This has been confirmed in our model system of cisplatin-sensitive versus cisplatin-resistant cell lines where the platinum accumulation of compound **5** was similar in both cell lines, suggesting that reduced active uptake mechanisms do not affect influx of compound **5**.

Cellular responses. To further explore the cytotoxicity effect of compound **5**, we evaluated its inhibition efficiency to cisplatin-sensitive A549 and cisplatin-resistant A549/CDDP cancer cell lines via cell growth inhibition, apoptosis and colony

JPET Fast Forward. Published on September 15, 2017 as DOI: 10.1124/jpet.117.243451
This article has not been copyedited and formatted. The final version may differ from this version.

forming assays (Fig. 5). Cells were incubated with 15 μM of chlorambucil, cisplatin, DN604 and compound **5**, respectively, in culture medium. The results in Fig. 5A right panel indicated that compound **5** exhibited better cytotoxic ability on cisplatin-resistant A549/CDDP cancer cells than cisplatin. To evaluate whether their cytotoxicity effects were associated with cell apoptosis, an Annexin V/PI staining was employed. Cancer cells were incubated with 15 μM of chlorambucil, cisplatin, DN604 and compound **5**, respectively, for 24 h. The results, shown in Fig. 5B, indicated that compound **5** could induce apoptosis much more effectively than cisplatin and DN604 in A549/CDDP cancer cells, while chlorambucil alone did not induce apoptotic changes, suggesting that a significant cytotoxicity effect of compound **5** was due to promoting cancer cell apoptosis.

The caspase-3 activity in cancer cells was determined at concentration of 15 μM of chlorambucil, cisplatin, DN604 and compound **5**, respectively, for 24 h. The cells incubated with compound **5** showed a high degree of caspase-3 activity compared to cisplatin and DN604 in A549/CDDP cancer cells (Fig. 5C). These findings indicated that compound **5** might induce higher level of caspase-dependent apoptosis than cisplatin in cisplatin-resistant cancer cells.

The CFA assay (CFA) is an extensively used and well-established method for testing chemotherapeutic agents *in vitro* (Li et al, 2009), reflecting the ability of chemotherapeutic agents to prevent the cell from dividing. To further detect the effect of cell proliferation inhibition of compound **5**, we used the colony forming assay to

JPET Fast Forward. Published on September 15, 2017 as DOI: 10.1124/jpet.117.243451
This article has not been copyedited and formatted. The final version may differ from this version.

compare the ability of compound **5** and cisplatin to prevent the proliferation of cisplatin-sensitive A549 and cisplatin-resistant A549/CDDP cancer cell lines. Cells were treated with 15 μM of chlorambucil, cisplatin, DN604 and compound **5**, respectively, for 7 days. As shown in Fig. 5D, fewer colonies apparently survived on the plates exposed to compound **5** than those on the plates treated with cisplatin. Thus, compound **5** was more effective than cisplatin in overcoming the drug resistance of A549/CDDP cancer cells.

Compound 5 induced cell cycle arrest, disturbed Ca^{2+} and K^{2+} homeostasis and decreased ΔΨm. Since antitumor platinum drugs can usually block the DNA synthesis to induce cell apoptosis, the effect on cell cycle progression of compound **5** was examined. Cisplatin-sensitive A549 and A549/CDDP cancer cells were treated with 15 μM of chlorambucil, cisplatin, DN604 and compound **5**, respectively, for 24 h, then cell cycle distribution was determined. It has been reported that cisplatin can arrest the cells at the S phase. In our experiment, compared with the untreated cells, the number of A549 and A549/CDDP cancer cells in the S phase increased from 32.75% to 47.53% and 32.95% to 38.62% when treated with cisplatin (Fig. 6A). And chlorambucil also arrested the cells at the S phase (35.17% and 36.28%), slightly weaker than cisplatin. As for compound **5**, the number of cells arrested at the S phase increased to 61.75% in A549/CDDP cancer cells, the best among the groups. The results proved that compound **5** still acted on DNA and contributed to the cycle

JPET Fast Forward. Published on September 15, 2017 as DOI: 10.1124/jpet.117.243451
This article has not been copyedited and formatted. The final version may differ from this version.

arresting of the cisplatin-resistant cancer cells. Additionally, it was obvious that chlorambucil can strengthen the ability of the Pt(IV) complex to arrest the cell cycle.

As K^+ efflux has frequently been observed in apoptosis, we measured the extracellular K^+ concentrations in treated and untreated cancer cells (Kondratskyi et al., 2015). As displayed in Fig. 6B, compound **5** elicited a gradual release of K^+ to the extracellular environment, with peak extracellular concentrations (increased by 69.27% and 55.69% in A549 and A549/CDDP, respectively) observed at 4 h after treatment. On the other hand, extracellular K^+ concentrations increased by 89.75% and 27.37% in the cisplatin-treated A549 and A549/CDDP cells after 4 h. These results indicated that compound **5** gradually increased K^+ leakage compared to cisplatin, supporting the idea that compound **5** might cause apoptosis higher than cisplatin in A549/CDDP cancer cells.

Ca^{2+} particularly plays an important role in apoptosis (Pinton et al., 2015), whose uptake by mitochondria is related to the activation of apoptotic factors, like caspase and cytochrome c (Foti et al., 2012). Thus, we investigated levels of cytosolic and mitochondrial Ca^{2+}. Fura-2AM reacts with cytosolic Ca^{2+} and Rhod-2AM, which easily enters mitochondria because of its cations and reacts with mitochondrial Ca^{2+}. The results in Fig. 6C showed that compound **5** induced an increase in cytosolic and mitochondrial Ca^{2+}, compared to cisplatin-treated cells. As compound **5** causes mitochondrial Ca^{2+} accumulation, the loss of $\Delta\Psi m$ following breakdown of ion homeostasis can be induced. Considering that loss in $\Delta\Psi m$ is an important

JPET Fast Forward. Published on September 15, 2017 as DOI: 10.1124/jpet.117.243451
This article has not been copyedited and formatted. The final version may differ from this version.

pro-apoptotic index for early apoptosis, we chose a mitochondria-specific and voltage-dependent fluorescent probe, JC-1, to observe whether there was loss in ΔΨm. The results from flow cytometry shown that compound **5** could make ΔΨm decrease mostly compared with cisplatin (Fig. 6D). Since ATP production is a significant consequence attributed to the dysfunction of mitochondrial energy production, we measured intracellular ATP levels after compound **5** treatment. As shown in Fig. 6E, the ATP level in cells treated with compound **5** at 15 μM decreased to 12.83%, 7.96% of untreated A549 and A549/CDDP cancer cells, respectively, which was 5.74% and 23.91% lower than that of cisplatin-treated cells.

Compound 5 induced ROS and H_2O_2 generation of cancer cells. Reactive oxygen species (ROS) play important roles in a variety of physiological and pathophysiological processes (Finkel and Holbrook, 2000). Previous explorations reported that excess accumulation of ROS is associated with disruption of mitochondrial membrane potential (MMP), therefore triggering a series of mitochondria-associated events including apoptosis (Park et al., 2005). Moreover, there has been a report that metal complexes may cause the accumulation of reactive oxygen species (ROS) and DNA damage, resulting in cell arrest and apoptosis eventually (Deng et al., 2015). Thus, the generation of ROS was investigated to further analyze the anticancer mechanism of compound **5**. Cells were treated with 15 μM of chlorambucil, cisplatin, DN604 or compound **5**, respectively, for 6 h, stained

JPET Fast Forward. Published on September 15, 2017 as DOI: 10.1124/jpet.117.243451
This article has not been copyedited and formatted. The final version may differ from this version.

with 10 mM H_2DCFDA for 30 min and then analyzed by flow cytometry. After incubation, cisplatin did not show apparent effect on the level of ROS compared with the control group in A549/CDDP, while the level of ROS cells increased after the treatment with chlorambucil as expected. As for compound **5**, the ROS level increased (Fig. 6F**)**, which was definitely higher than other groups in cisplatin-resistant A549/CDDP cells.

Taking into account that among all ROS and other oxygen-derived free radicals, H_2O_2 has been recently suggested to act as a central player in signal transduction pathways (Halliwell and Cross, 1994), we evaluated H_2O_2 generation by a fluorometric assay in cancer cells incubated in the presence of 15 μM of chlorambucil, cisplatin, DN604 and compound **5**, respectively. H_2O_2 measurement was carried out after 2 h incubations with chlorambucil and cisplatin, DN604 and compound **5**, respectively. The production of H_2O_2 was significantly higher in cancer cells incubated with compound **5** than those in cells treated with chlorambucil along and cisplatin in cisplatin-resistant A549/CDDP cancer cells (Fig. 6G). The results strongly suggested that compound **5** could induce increased intracellular oxidative stress compared with chlorambucil and cisplatin, thus triggering cisplatin-resistant cancer cell apoptotic pathways.

Biomarkers of DNA damage. Following the treatment of compound **5**, we measured intracellular GSH levels in cisplatin-sensitive and cisplatin-resistant cancer

JPET Fast Forward. Published on September 15, 2017 as DOI: 10.1124/jpet.117.243451
This article has not been copyedited and formatted. The final version may differ from this version.

cells. As illustrated in Fig. 7A, the cisplatin-resistant A549/CDDP cancer cells expressed higher levels of intracellular GSH than the cisplatin-sensitive A549 cancer cells. When A549/CDDP cancer cells were treated in 800 ng/ml cisplatin for 4 h, intracellular GSH levels increased. While treating with compound **5**, however, intracellular GSH levels did significantly reduce. These results proved that compound **5** reduces intracellular GSH levels to improve active platinum delivery to the DNA to interact with cellular components and causes severe DNA damage (Foti et al., 2012; You et al., 2009). As shown in Fig. 7B, compound **5** produced dramatically prominent tails induced by SSBs, DSBs and active DNA cross-links excision breaks in contrast to cisplatin in three major parameters (tail length, tail moment, olive tail moment). The data obviously shown that compound **5** could effectively cause DNA damage in A549 and A549/CDDP cells compared with DN604 and cisplatin alone, thereby leading to cancer cell apoptosis.

Because the chlorambucil-conjugated Pt(IV) hybrid could accumulate in both the mitochondria and nucleus in cancer cells, the effects of DNA damage delivered by cisplatin and compound **5** on the two genomes were determined by PCR amplification of DNA. A 17.7 kb segment of nDNA at the b-globin gene and an 8.9 kb fragment of mtDNA were used for detection following cancer cells treated with cisplatin and compound **5**. As shown in Fig. 7C, cisplatin primarily damaged nDNA with a few mitochondrial lesions, whereas compound **5** caused a significant reduction of mitochondrial genome amplification with similar effect on the nuclear genome. Thus,

JPET Fast Forward. Published on September 15, 2017 as DOI: 10.1124/jpet.117.243451
This article has not been copyedited and formatted. The final version may differ from this version.

compound **5** mainly damaged nDNA and mtDNA, although most intracellular Pt accumulated in the nucleus.

In order to detect the DSBs induced by the measured samples, we determined the phosphorylated histone H2AX (γH2AX), the known earliest detectable marker of DSB. Two cancer cells were treated with the measured samples at the fixed concentration of 15 μM for 12 h, respectively. As shown in the flow cytometry assessment of γH2AX in A549 and A549/CDDP treated with corresponding samples (Fig. 7D), compound **5** produced increased level of discrete γH2AX foci compared with cisplatin for 12 h, proving that the extent of DSBs increased apparently in two cancer cells, especially in the cisplatin resistant cancer cells. However, such changes were not apparently observed after the treatment of cisplatin. Under these conditions, the DNA damage of DSBs and SSBs revealed the possibility that the increased level of DSBs induced by compound **5** is much higher than that of SSBs in cancer cells while compared with cisplatin. The result implied that the most lethal attack of DSBs plays an important role in compound **5**-triggerred serious cell apoptosis which probably accounts for the improved cellular uptake of Pt.

Compound 5 repressed MRE11-RAD50-NBS1 complex protein expression in DSB repair response. In order to reveal the mechanisms underlying the enhanced cytotoxicity and the resistance prevention, compound **5** was studied to learn whether it could reduce the activation of DNA repair response including activation of DSB

JPET Fast Forward. Published on September 15, 2017 as DOI: 10.1124/jpet.117.243451
This article has not been copyedited and formatted. The final version may differ from this version.

repair protein MRE11-RAD50-NBS1(MRN) complex within nucleus. Treatment of A549/CDDP cells with 15 μM compound **5** for 24 h led to a dramatically decrease in the expression of MRN complex protein to the damaged DNA compared with cisplatin (Fig. 8A). The results revealed that compound **5** could inhibit MRN complex-induced DSB repair caused by its ability of increasing cellular uptake of Pt compared with those of cisplatin.

Compound 5-induced suppression of DSB repair could be mimicked in MRN-deficient cells. Activation of DSB repair protein MRE11-RAD50-NBS1(MRN) complex suggested an important role of MRN complex to DSBs. The key subunit of the MRN complex, MRE11, interacts with PIH1D1 and contains additional protein-protein interaction domains important for MRN function in the DDR. The MRE11 C-terminal part contains two potential DNA-binding domains and a glycine–arginine-rich motif, involved in the regulation of MRE11 nuclease activity and DNA binding (Dery et al., 2008; Yu et al., 2012).

To study the role of MRE11 played in compound **5**-induced suppression of DSB repair, we transfected wild-type and siMRE11 to A549/CDDP cancer cells, and monitored the repair kinetics of DSB via imaging the discrete γH2AX foci in A549/CDDP cancer cells. The similar repair kinetics of DSB observed in A549/CDDP cancer cells (Fig. 8B) indicated that MRE11 is necessary for the inhibition of DSB repair induced by compound **5**. Meanwhile, the suppression of DSB repair induced by

JPET Fast Forward. Published on September 15, 2017 as DOI: 10.1124/jpet.117.243451
This article has not been copyedited and formatted. The final version may differ from this version.

compound **5** could be enhanced in MRE11$^{-/-}$ cells (Fig. 8C), demonstrating that the deficient MRE11 could mimic the inhibitory ability of compound **5** in DSB repair. These data implied a critical role of MRE11 in compound **5**-induced DSB suppression and resistance prevention.

The key role of CK2 in compound 5-mediated MRE11 activation and reversed cisplatin resistance in A549/CDDP cancer cells. MRE11 could directly interact with PIH1D1, which is required for the assembly of MRN complex. The MRE11-PIH1D1 interaction is dependent on casein kinase 2 (CK2) phosphorylation of two acidic sequences within the MRE11 C terminus containing serines 558/561 and 688/689. Consistent with the findings, depletion of CK2 resulted in MRE11 destabilization and decreased assembly of the MRN complex, leading to hinder DNA-damage repair processes (Morgen et al., 2017). We investigated whether compound **5** directly inhibits CK2 activity. The results from the CK2 kinase assay indicated that compound **5** significantly suppressed CK2 activity (Fig. 8D). As shown in Fig. 8E, transfection of either CK2α or CK2β subunits or both gives rise to the expected patterns with the anti-Myc antibody. A 75, 18, and 109% increase in CK2 activities from A549/CDDP cells that were transfected with CK2α or CK2β or both, and observed compared with the control. Results of the MRE11 protein expression assay in Fig. 8F exhibited 28 and 75% increases in cells transfected of CK2α or both. These data provide evidence that both of CK2α and CK2β are required for MRE11 activation. The results in Fig.

JPET Fast Forward. Published on September 15, 2017 as DOI: 10.1124/jpet.117.243451
This article has not been copyedited and formatted. The final version may differ from this version.

8G indicated that the increased MRE11 protein expression could be inhibited in compound **5**-treated A549/CDDP cancer cells co-transfected with CK2α and CK2β. The results from the CFA assay, shown in Fig. 8H, indicated that the increased colonies survived on the plates exposed to compound **5** in the cells co-transfected with CK2α and CK2β, compared to empty vector. Moreover, the cell death of A549/CDDP treated with compound **5** was reduced in the presence of CK2α and CK2β subunits (Fig. 8I). These results demonstrated that CK2α/β was involved in compound **5** suppression of MRE11 activation in A549/CDDP cancer cells.

***In vivo* antitumor activity.** *In vivo* antitumor efficacy of compound **5** on the A549/CDDP tumor xenograft mice model was assayed together with cisplatin, DN604 and chlorambucil. Compound **5** (dosed intravenously at 5 mg/kg once a week), cisplatin (dosed intravenously at 5 mg/kg once a week), DN604 (dosed intravenously at 5 mg/kg once a week), chlorambucil (dosed intravenously at 5 mg/kg once a week) were conducted into four nude mice groups. The tumor volumes, measured using vernier calipers every two days in a period of 21 days, indicated that compound **5** can effectively inhibit the tumor growth (Fig. 9A). At the end of 21 days period, the tumor weight was measured to detect the antitumor activity of these measured groups. The tumor growth inhibition rate of compound **5** reached 75.81%, while that of cisplatin at the same dose as compound **5** was only 22.58%. Compound **5** significantly exhibited the highest tumor growth inhibition among the tested samples (Fig. 9B). Because

JPET Fast Forward. Published on September 15, 2017 as DOI: 10.1124/jpet.117.243451
This article has not been copyedited and formatted. The final version may differ from this version.

cisplatin is well known for its toxic effects on the mean bodyweights of treated animals, the bodyweights of mice treated with these drugs were assayed. The results in Fig. 9C illustrated that a bodyweight increase of the mice was observed in the compound **5** group, while a continuous bodyweight decrease of the mice was seen in the cisplatin group. The mice treated with the tested samples were selected for histological analyses. As a result, there was no obvious change, pathological injury and inflammation infiltration in major organs of liver and kidney between control and compound **5**-treated group (Fig. 9D). The HE staining of slices from the tissues and Pt uptake demonstrated that compound **5** had hardly toxic effect on normal tissues compared to cisplatin (Figs. 9D and 9E). All these data proved that compound **5** exhibits significant antitumor activity with nearly no toxic effect on treated animals in contrast to cisplatin, DN604 and chlorambucil.

Pharmacokinetics. The stability of the hybrid in blood is significantly important for its clinical application. Therefore, we investigated the stability of compound **5** in rat plasma using ICP-MS. Fresh rat plasma was added with a DMF solution of compound **5** (50 μM). Following the incubation for 0, 2, 4 and 8 h at 37 ℃, the Pt content was measured by ICP-MS. The results in Fig. 9F showed that the Pt content decreased to 31.37% after 8h incubation. The result reveals the half-life of compound **5** in rat plasma to be 4.59 h, which is significantly longer than that of cisplatin ($t_{1/2}$ ~ 30.24 min). The data contributes to the promising stability of compound **5** in rat

JPET Fast Forward. Published on September 15, 2017 as DOI: 10.1124/jpet.117.243451
This article has not been copyedited and formatted. The final version may differ from this version.

plasma. The pharmacokinetic profile of compound **5** was also performed in contrast to cisplatin. It was noticed that cisplatin and compound **5** followed a two-compartment pharmacokinetic model, which was based on the residual sum of squares and minimum Akaike's information criterion (AIC) value. The results in Fig. 9G demonstrated the Pt concentration-time profiles in rat plasma, revealing the half-life of compound **5** ($t_{1/2}$ ~ 5.08 h) to be 2.63-folds increased compared to cisplatin ($t_{1/2}$ ~ 1.93 h). Although rapid elimination of Pt via blood circulation occurred in both cisplatin and compound **5**-treated groups, changes of these preparations were significantly different and significant increased release time was observed in the compound **5**-treated group. Notably, compound **5** had a longer blood retention as compared to cisplatin, which could dramatically promote Pt accumulation in tumor tissues in the compound **5**-treated group. The results could be attributed to the biodistribution of compound **5** in normal tissues as well as retention in blood circulation. Hence, compound **5** with longer circulation time could significantly improve *in vivo* pharmacokinetics of the corresponding Pt(II) drug and increase their bioavailability.

Upon above all the study, compound **5**, possessing significant antitumor activity via reversing platinum resistance and exhibiting nearly no toxic effect, has a potential promise to be a platinum-based anticancer drug candidate.

Disscussion

DNA-damaging chemotherapy is effective in the treatment of advanced cancer with a high survival benefit. However, DNA-damaging drugs as cisplatin induced resistance remains a major obstacle to the clinical management of human solid tumor, resulting in its relapse and metastasis. As the development of platinum analogues with better therapeutic effects, carboplatin showed fewer side effects with an antitumor activity similar to that of cisplatin, but shows cross-resistance to cisplatin resistant cancer cells (Sorenson and Eastman, 1998). To further overcome the acquired resistance associated with platinum based therapies, we concomitantly developed a new Pt(II) drugs DN604, a carboplatin analogue containing 3-oxocyclobutane-1,1-dicarboxylate (OCBDC) as a leaving group which has been successful in overcoming cisplatin resistance in cancer cells. Thus, DN604 can be applied as one of the leading treatment options for unresponsive cisplatin-based chemotherapy in human cancer.

The lack of sensitivity to chlorambucil treatment observed in human cancer cell lines is typical. In both breast and pancreatic cancers, DSB repair mechanisms have been linked with resistance to DNA-targeted therapies (Mao et al., 2009; Li et al., 2012). Moreover, the primary mechanism of chlorambucil cytotoxicity involves the formation of N7G cross-links (Kondo et al., 2010), inhibit DNA synthesis and cause DSBs. Repair of persistent DNA damage induced by chlorambucil required the engagement of multiple DSB repair mechanisms that are often up-regulated in

JPET Fast Forward. Published on September 15, 2017 as DOI: 10.1124/jpet.117.243451
This article has not been copyedited and formatted. The final version may differ from this version.

chlorambucil resistant breast and pancreatic cancer tumors (Shaheen et al., 2011). So, the significant therapeutic efficacy that are achieved while combining chlorambucil with agents that prevent DSB repair such as PARP inhibitors (Evers et al., 2010). In this work, we combined DN604 with a chlorambucil unit to detect its therapeutic effects on cisplatin resistant tumor both *in vitro* and *in vivo*. Definitely, the hybrids were prepared via introducing the chlorambucil moiety to the axial position of the corresponding Pt(II) complexes via a linker group to deliver Pt and chlorambucil to tumor tissue and stay there.

At nearly half concentrations and dosages of Pt and chlorambucil, compound **5** improved the ability of the drugs to kill drug resistant A549/CDDP cells and tumor xenograft mice model. In our study, compound **5** exhibited the dramatically high level of DNA damage which was not found in cisplatin and chlorambucil in the comet assay. The results revealed that compound **5** could increase the sensitivity of the tumor cells to cisplatin and chlorambucil, and reverse drugs-mediated resistance via increasing their cellular uptake and suppressing MRE11-RAD50-NBS1(MRN) complex in DSB repairs. These results proved that such a conjugate between DN604 and the chlorambucil unit could not only enhance their synergistic anticancer effect, but also strengthen the abilities of damaging DNA and inhibiting MRN complex-induced DSB repair.

DSBs can be recognized by the MRE11-RAD50-NBS1(MRN) complex, which is a member of the SMC family containing ATPase domains and associates with the

JPET Fast Forward. Published on September 15, 2017 as DOI: 10.1124/jpet.117.243451
This article has not been copyedited and formatted. The final version may differ from this version.

DNA ends of the DSBs, thus promoting the activation of ATM and the preparation of DNA for HR. In addition to stabilizing DNA ends, MRE11 has endonuclease and exonuclease activities important for the initial steps of DNA end resection that is essential for HR, as described below (Williams et al., 2007). MRE11 directly interacts with PIH1D1, which is required for the assembly of MRN complex. The MRE11-PIH1D1 interaction is dependent on casein kinase 2 (CK2) phosphorylation of two acidic sequences within the MRE11 C terminus containing serines 558/561 and 688/689. Moreover, the PIH1D1 phospho-binding domain PIH-N is required for association with MRE11 phosphorylated by CK2. Thus, depletion of CK2 resulted in MRE11 destabilization and affected DNA-damage repair processes. The results showed that the inhibition of DSB repair induced by compound **5** could be enhanced in MRE11$^{-/-}$ cisplatin resistant cancer cells (Fig. 8C), demonstrating a critical role of MRE11 in compound **5**-mediated DSB repair suppression and resistance prevention, which is a novel target to augment efficacy of cancer therapies. Meanwhile, the effects of compound **5** on CK2-mediated MRE11 activity were observed in the cisplatin-resistant A549/CDDP cancer cells.

During DSB repair, PARP1 is thought to mediate the initial accumulation of the MRN complex to DSBs in a γH2AX- and MDC1-independent manner (Haince et al., 2008). Moreover, PARP1 plays an initial role in the DSBs by facilitating ATM activation, while the delayed phosphorylation of ATM substrates in the absence of PARP1 following treatment with DNA-damaging agents (Haince et al., 2007). The

JPET Fast Forward. Published on September 15, 2017 as DOI: 10.1124/jpet.117.243451
This article has not been copyedited and formatted. The final version may differ from this version.

effect of compound **5** on PARP1-mediated accumulation of MRN complex in DSB repair should be determined significantly in further study.

Compared with known Pt(IV) complexes which could overcome cisplatin resistance as mentioned in previous reports (Wang et al., 2016; Li et al., 2015; Pichler et al., 2015), compound **5** exhibited lower drug resistance factor (RF) and improved *in vivo* safety. To sum up, introduction of chlorambucil to the Pt(IV) complexes derived from the Pt(II) complexes, DN604 and DN603, has resulted in the formation of two novel Pt(IV) compounds. Among which, compound **5** presented potent cytotoxicity against two pairs of cisplatin sensitive (SGC-7901 and A549) and cisplatin resistant (SGC-7901/CDDP and A549/CDDP) cell lines. Compound **5** was found to be highly accumulated in tumor cells for its high lipophilicity and stability as a Pt(IV) complex, which can be readily reduced by ascorbic acid to release active drugs, DN604 and chlorambucil. Its enhanced cellular uptake of Pt and subsequently platinated DNA can cause extensive DSBs damage, inducing cell cycle arrest and apoptosis. With the increased extent of cellular uptake following the treatment of compound **5** with the cancer cells, severe DNA damage was detected as DSBs, while in contrast most SSBs happened in cisplatin-treated cancer cells. The coordinated chlorambucil to the platinum moiety was able to significantly inhibit DSB repair with MRE11-RAD50-NBS1(MRN) complex, which related to the resistance mediated by DNA-damaging platinum-based chemotherapy drugs. The results imply that compound **5** could increase the sensitivity of the tumor cells to DN604 and reverse

JPET Fast Forward. Published on September 15, 2017 as DOI: 10.1124/jpet.117.243451
This article has not been copyedited and formatted. The final version may differ from this version.

cisplatin-mediated resistance via increasing its cellular uptake and suppressing CK2-mediated MRE11-RAD50-NBS1(MRN) complex in DSB repair. The study indicated that compound **5** possessed significant antitumor activity and had hardly toxicity compared with cisplatin and chlorambucil, revealing an effective strategy to promote the anticancer potency of the DNA-damaing drugs for exploring multiple targeting cancer therapies.

Conflict of interest

None declared.

Acknowledgments

We want to express our gratitude to the Priority Academic Program Development of Jiangsu Higher Education Institutions for the construction of fundamental facilities.

Authorship Contributions

Participated in research design: Shaohua, Feihong

Conducted experiments: Feihong, Xiufeng

Performed data analysis: Gang, Xiaodong

Wrote or contributed to the writing of the manuscript: Shaohua, Feihong

JPET Fast Forward. Published on September 15, 2017 as DOI: 10.1124/jpet.117.243451
This article has not been copyedited and formatted. The final version may differ from this version.

References

Arduino DM, Esteves AR, Domingues AF, Pereira CM, Cardoso SM, Oliveira CR (2009) ER-mediated stress induces mitochondrial-dependent caspasesactivation in NT2 neuron-like cells. *Bmb Rep* 42:719-724.

Alonso-Monge R, Carvaihlo S, Nombela C, Rial E, Pla J (2009) The Hog1 MAPkinase controls respiratory metabolism in the fungal pathogen. *Candidaalbicans Microbiol* 155:413-423.

Cobo M, Isla D, Massuti B, Montes A, Sanchez JM, Provencio M, Vinolas N, Paz-Ares L (2007) Customizing cisplatin based on quantitative excision repair cross-complementing 1 mRNA expression: a phase III trial in non small-cell lung cancer. *J Clin Oncol* 25:2747-2754.

Chabner BA, Bertino J, Cleary J, Ortiz T, Lane A, Supko JG, Ryan D (2011) Cytotoxic agents. In goodman & gilman's pharmacologic basis of therapeutics:, 12th ed.; Brunton LL CB, Knollmann BC, ed.; McGraw-Hill: New York, Chapter 61.

Chen FH, Zhang LB, Qiang L, Yang Z, Wu T, Zou MJ, Tao L, You QD, Li ZY, Yang Y (2010) Reactive oxygen species-mitochondria pathway involved in LYG-202-induced apoptosis in human hepatocellular carcinoma HepG2 cells. *Cancer Lett* 296:96-105.

Cannavo E, Cejka P (2014) Sae2 promotes dsDNA endonuclease activity within Mre11-Rad50-Xrs2 to resect DNA breaks. *Nature* 514:122-125.

Chen FH, Huang XC, Wu M, Gou SH, Hu WW (2017) A CK2-targeted Pt(IV) prodrug to disrupt DNA damage response. *Cancer Lett* 385:168-178.

Chen FH, Lu N, Zhang HW, Zhao L, He LC, Sun HP, You QD, Li ZY, Guo QL (2012) Augments tumor necrosis factor-α-induced apoptosis via attenuating CK2-dependent NF-κB pathway in HepG2 cells. *Mol Pharmacol* 82:958-971.

Dhar S, Kolishetti N, Lippard SJ, Farokhzad OC (2011) Targeted delivery of a cisplatin prodrug for safer and more effective prostate cancer therapy *in vivo*. *Proc Natl Acad Sci* 108:1850-1855.

Deng ZQ, Yu LL, Chen TF (2015) A selenium-containing ruthenium complex as a cancer radiosensitizer, rational design and the important role of ROS-mediated signalling. *Chem Commun* 51:2637-2640.

Dery U, Coulombe Y, Rodrigue A, Stasiak A, Richard S, Masson JY (2008) A glycinearginine domain in control of the human MRE11 DNA repair protein. *Mol Cell Biol* 28:3058-3069.

Evers B, Schut E, van der Burg E, Braumuller TM, Egan DA, Holstege H, Edser P, Adams DJ, Wade-Martins R, Bouwman P, Jonkers J (2010) A high-throughput pharmaceutical screen identifies compounds with specific toxicity against BRCA2-deficient tumors. *Clin Cancer Res* 16:99-108.

Fonseca SB, Pereira MP, Mourtada R, Gronda M, Horton KL, Hurren R, Minden MD, Schimmer AD, Kelley SO (2011) Rerouting chlorambucil to mitochondria combats drug deactivation and resistance in cancer cells. *Chem Biol* 18:445-453.

Fousteris MA, Koutsourea AI, Arsenou ES, Papageorgiou A, Mourelatos D, Nikolaropoulos SS (2006) Structure–anti-leukemic activity relationship study of B-and D-ring modified and non-modified steroidal esters of chlorambucil. *Anti-Cancer Drugs* 17:511-519.

Foti J, Devadoss B, Winkler J, Collins J, Walker G (2012) Oxidation of the guanine nucleotide pool underlies cell death by bactericidal antibiotics. *Science* 336: 315-319.

Finkel T, Holbrook NJ (2000) Oxidants, oxidative stress and the biology of ageing. *Nature* 408:239-247.

Hemminki K, Ludlum DB (1983) Covalent modification of DNA by antineoplastic agents. *J Natl Cancer Inst* 73:1021-1028.

Hansson J, Lewensohn R, Ringborg U, Nilsson B (1987) Formation and removal of DNA cross-links induced by melphalan and nitrogen mustard in relation to drug-induced cytotoxicity in human melanoma cells. *Cancer Res* 47:2631-2637.

Huang XC, Huang RZ, Gou SH, Wang Z, Liao Z, Wang H (2016) Combretastatin A-4 analogue: adual-targeting and tubulin inhibitor containing antitumor Pt(IV) moiety with a unique mode of action. *Bioconjugate Chem* 27:2132-2148.

Hall MD, Okabe M, Shen DW, Liang XJ, Gottesman MM (2008) The role of cellular accumulation in determining sensitivity to platinum-based chemotherapy. *Annu Rev Pharmacol Toxicol* 48:495-535.

Halliwell B, Cross C (1994) Oxygen-derived species: their relation to human disease

and environmental stress. *Environ Health Perspect* 102:5-12.

Haince JF, McDonald D, Rodrigue A, Dery U, Masson JY, Hendzel MJ, Poirier GG (2008) PARP1-dependent kinetics of recruitment of MRE11 and NBS1 proteins to multiple DNA damage sites. *J Biol Chem* 283:1197-1208.

Haince JF, Kozlov S, Dawson VL, Dawson TM, Hendzel MJ, Lavin MF, Poirier GG (2007) Ataxia telangiectasia mutated (ATM) signaling network is modulated by a novel poly(ADP-ribose)-dependent pathway in the early response to DNA-damaging agents. *J Biol Chem* 282:16441-16453.

Ishida S, Lee J, Thiele DJ, Herskowitz I (2002) Uptake of the anticancer drug cisplatin mediated by the copper transporter ctr1 in yeast and mammals. *Proc Natl Acad Sci USA* 99:14298-142302.

Kohn KW (1980) Molecular aspects of anti-cancer drug action; Macmillan publishers: London, 233-282.

Kohn KW, Hartley JA (1987) Mattes WB. Mechanisms of DNA sequence selective alkylation of guanine-N7 positions by nitrogen mustards. *Nucl Acids Res* 37:1799-1800.

Klein AV, Hambley TW (2009) Platinum drug distribution in cancer cells and tumors. *Chem Rev* 109:4911-4920.

Kuo MT, Chen HH, Song IS, Savaraj N, Ishikawa T (2007) The roles of copper transporters in cisplatin resistance. *Cancer Metastasis Rev* 26:71-83.

Kondratskyi A, Kondratska K, Skryma R, Prevarskaya N (2015) Ion channels in the

regulation of apoptosis. *BBA* 1848:2532-2546.

Kondo N, Takahashi A, Ono K, Ohnishi T (2010) DNA damage induced by alkylating agents and repair pathways. *J Nucleic Acids* 2010:543531.

Li YH, Wang X, Pan Y, Lee DH, Chowdhury D, Kimmelman AC (2012) Inhibition of non-homologous end joining repair impairs pancreatic cancer growth and enhances radiation response. *PLoS One* 7:39588.

Li ZY, Cao X, Wang X, Guo QL, You QD (2009) Convenient synthesis of wogonin, a flavonoid natural product with extensive pharmacological activity. *Org Prep Proced Int* 41:327-330.

Li YL, Deng YB, Tian X, Ke HT, Guo M, Zhu AJ, Yang T, Guo ZQ, Ge ZS, Yang XL, Chen HB (2015) Multipronged design of light-triggered nanoparticles to overcome cisplatin resistance for efficient ablation of resistant tumor. *ACS Nano* 9:9626-9637.

Mao Z, Jiang Y, Liu X, Seluanov A, Gorbunova V (2009) DNA repair by homologous recombination, but not by nonhomologous end joining, is elevated in breast cancer cells. *Neoplasia* 11:683-691.

Morgen PV, Burdova K, Flower TG, O'Reilly NJ, Boulton SJ (2017) MRE11 stability is regulated by CK2-dependent interaction with R2TP complex. *Oncogene* 1-8.

Mao Z, Jiang Y, Liu X, Seluanov A, Gorbunova V (2009) DNA repair by homologous recombination, but not by nonhomologous end joining, is elevated in breast cancer cells. *Neoplasia* 11:683-691.

O'Grady S, Finn SP, Cuffe S, Richard DJ, O'Byrne KJ, Barr MP (2014)The role of DNA repair pathways in cisplatin resistant lung cancer. *Cancer Treat Rev* 40: 1161-1170.

Pathak RK, Marrache S, Choi JH, Berding TB, Dhar S (2014) The prodrug platin-A: simultaneous release of cisplatin and aspirin. *Angew Chem Int Edit* 126:1994-1998.

Pinton P, Giorgi C, Siviero R, Zecchini E, Rizzuto R (2015) Calcium and apoptosis: ER-mitochondria Ca^{2+} transfer in the control of apoptosis. *Oncogene* 27:6407-6408.

Park MT, Kim MJ, Bae S (2005) Phytosphingosine in combination with ionizing radiation enhances apoptotic cell death in radiation-resistant cancer cells through ROS-dependent and-independent AIF release. *Blood* 105:1724-1733.

Pichler V, Göschl S, Schreiber-Brynzak E, Jakupec MA, Galanski M, Keppler BK (2015) Influence of reducing agents on the cytotoxic activity of platinum(IV) complexes: induction of G2/M arrest, apoptosis and oxidative stress in A2780 and cisplatin resistant A2780cis cell lines. *Metallomics* 7:1078-1090.

Rosenberg B, VanCamp L, Trosko JE, Mansour VH (1969) Platinum compounds: a new class of potent antitumor agents. *Nature* 222:385-386.

Schipler A, Iliakis G (2013) DNA double-strand break complexity levels and their possible contributions to the probability for error-prone processing and repair pathway choice. *Nucl Acids Res* 41:7589-7605.

Siddiqui-Jain A, Drygin D, Streiner N, Chua P, Pierre F, O'Brien SE, Bliesath J, Omori M, Huser N, Ho C (2010) CX-4945, an orally bioavailable selective inhibitor of protein kinase CK2, inhibits prosurvival and angiogenic signaling and exhibits antitumor efficacy. *Cancer Res* 70:10288-10298.

Sorenson CM, Eastman A (1998) Mechanism of cis-diamminedichloroplatinum(II)-induced cytotoxicity: role of G2 arrest and DNA double-strand breaks. *Cancer Res* 48:4484-4488.

Valipour M, Sefidkouhi MAG, Eslamian S (2015) Surface irrigation simulation models: a review. *Int J Hydrol Science Technol* 5:51-70.

Williams GJ, Lees-Miller SP, Tainer JA (2010) Mre11-Rad50-Nbs1 conformations and the control of sensing, signaling, and effector responses at DNA double-strand breaks. *DNA Repair* 9:1299-1306.

Williams RS, Williams JS, Tainer JA (2007) MRE11-RAD50-NBS1 is a keystone complex connecting DNA repair machinery, double-strand break signaling, and the chromatin template. *Biochem Cell Biol* 85:509-520.

Wang ZG, Xu ZF, Zhu GY (2016) A platinum(IV) anticancer prodrug targeting nucleotide excision repair to overcome cisplatin resistance. *Angew Chem Int Ed* 55:15564.

Yannopoulos SI, Lyberatos G, Theodossiou N, Li W, Valipour M, Tamburrino A, Angelakis AN (2015) Evolution of water lifting devices (pumps) over the centuries worldwide. *Water* 2015:5031-5036.

You Q, Li Z, Huang C, Yang Q, Wang X, Guo Q, Chen X, He X, Li T, Chern J (2009) Discovery of a novel series of quinolone and naphthyridine derivatives as potential topoisomerase I inhibitors by scaffold modification. *J Med Chem* 52:5649-5661.

Yu Z, Vogel G, Coulombe Y, Dubeau D, Spehalski E, Hebert J (2012) The MRE11 GAR motif regulates DNA double-strand break processing and ATR activation. *Cell Res* 22:305-320.

Zhao J, Gou SH, Liu FF (2014) Potent anticancer activity and possible low toxicity of platinum(II) complexes with functionalized 1,1-cyclobutanedicarboxylate as a leaving ligand. *Chem-Eur J* 20:15216-15225.

Footnotes

Feihong Chen and Gang Xu contributed equally to this article.

We are grateful to the National Natural Science Foundation of China [grant 21571033 and 81503099] for financial aids to this work. The research was also supported by Jiangsu Province Natural Science Foundation [grant BK20150643]. The authors would like to thank the Fundamental Research Funds for the Central Universities [project 2242016k30020] for supplying basic facilities to our key laboratory. Qin is grateful to the Innovation Program of Jiangsu Province Postgraduate Education [project KYLX15_0128].

Legends for Figures

Fig. 1. Chemical structures of mentioned compounds and Pt(IV) complexes

Fig. 2. ^{1}H (**A**), ^{13}C NMR (**B**) and ESI-MS (**C**) spectra of compound **5**.

Fig. 3. ^{1}H (**A**), ^{13}C NMR (**B**) and ESI-MS (**C**) spectra of compound **6**.

Fig. 4. Reactions of compound **5** with DNA by reduction and the cellular uptake of Pt in cisplatin-sensitive and cisplatin-resistant cancer cells. (**A**) The different Pt/nucleotide ratios and time of DNA platination. All the reactions were conducted with 0.01mg/mL DNA in 10 mM $NaClO_4$ in 10 mM phosphate buffer (pH=7.4) at 37℃ for 24 h and then add 0.04 mg/mL EtBr before the fluorescence measurements with the excitation wavelength of 546 nm and the emission wavelength of 590 nm. (**B**) The cellular uptake of measured compounds in cancer and normal cells at 37 ℃ and 4 ℃. (**C**) The accumulation of the measured compounds in mitochondria, lysosomes and nucleus of different cancer cells. (**D**) Western blot analysis of Ctr1 protein in different cancer cells; 25 μg protein extract (lanes 1, 6), 50 μg protein extract (lanes 2, 7), 75 μg (lanes 3, 8), 100 μg protein extract (lanes 4, 9) and 125 μg protein extract (lanes 5, 10) are separated on a 12 % polyacrylamide gel. Densitometric analysis was performed to determine the relative ratios of each protein. (**E**) Platinum accumulation of cisplatin and **5** in different cancer cells. Cells are pre-treated with the indicated concentrations of tetrathiomolybdate

JPET Fast Forward. Published on September 15, 2017 as DOI: 10.1124/jpet.117.243451
This article has not been copyedited and formatted. The final version may differ from this version.

for 24 h, followed by a 2h treatment with 15 μM cisplatin or **5**. All results are representative of at least three independent experiments and shown as the mean ± S.D. **P* < 0.05, ***P* < 0.01 compared with control group.

Fig. 5. Cellular responses of chlorambucil, cisplatin, DN604 and compound **5** in A549 and A549/CDDP cells. All the samples were used at the fixed concentration of 15 μM for 24h. (**A**) The inhibitory effects of measured samples against SGC-7901 and SGC-7901/CDDP, A549 and A549/CDDP cancer cells were detected by MTT assay. After treatment with various concentrations of cisplatin, DN604 and compound **5** for 24 h, growth inhibition was assessed. (**B**) The antiproliferative effects of the measured compounds. (**C**) Apoptosis inducing property of the measured samples by Annexin V-FITC/PI staining of cancer cells. The Y-axis shows the PI-labeled population and the X-axis shows FITC-labeled Annexin V-positive cells. (**D**) Analysis of caspase-3 activation in cancer cells following the treatment of measure compounds. (**E**) Long-term colony formation assays of A549 and A549/CDDP cells. Cells were grown in the presence of the measured compounds for 7 days. For each cell line, all dishes were fixed at the same time, stained and analyzed. Results are representative of at least three independent experiments and shown as the mean ± S.D. **P*<0.05, ***P*<0.01 compared with control group.

Fig. 6. Compound **5** induces cell death and cell cycle changes in A549 and A549/CDDP cancer cells. (**A**) Cell cycle analysis upon exposure to

JPET Fast Forward. Published on September 15, 2017 as DOI: 10.1124/jpet.117.243451
This article has not been copyedited and formatted. The final version may differ from this version.

compound **5**. A549 and A549/CDDP cancer cells exposed to the measured compounds for 72 h were stained with propidium iodide and subjected to flow cytometry analysis. Analysis of K^+ and Ca^{2+} levels following treatment with measured samples. (**B**) The relative amounts of extracellular K^+ were measured every 1 h. (**C**) Spectrofluorophotometric analysis of cytosolic and mitochondrial Ca^{2+} levels using Fura-2AM and Rhod-2AM, respectively. The mitochondrial membrane potential (**D**) and the intracellular ATP (**E**) decreased in compounds-treated A549 and A549/CDDP cancer cells. (**D**) Cells were exposed to chlorambucil, cisplatin, DN604 and compound **5** (15 μM) for 24 h, stained with JC-1 and visualized under an inverted fluorescence microscope. Red fluorescence of JC-1 dimers was present in the cell areas with high MMP, while green fluorescence of JC-monomers was prevalent in the cell areas with low MMP. Normalized JC-1 fluorescence change analyzed by flow cytometry. The median fluorescence intensity of each treatment group was normalized to the control group. (**E**) Cells were treated with chlorambucil, cisplatin, DN604 and compound **5** (15 μM), for 12 h and then the intracellular ATP was detected. (**F**) Intracellular ROS were measured by flow cytometry after 10 μM DCFH-DA staining. Geometric mean of fluorescence intensity values were calculated and compared to that in DMSO controls. (**G**) Cells were exposed to 15 μM chlorambucil, cisplatin, DN604 and compound **5**, then H_2O_2 level was

JPET Fast Forward. Published on September 15, 2017 as DOI: 10.1124/jpet.117.243451
This article has not been copyedited and formatted. The final version may differ from this version.

measured. Values are means ± SD for at least three independent experiments performed in triplicate (*P < 0.05 and **P < 0.01 compared with vehicle control).

Fig. 7. Intracellular GSH concentrations and DNA damage of the measured compounds. (**A**) A549 and A549/CDDP cells were incubated with chlorambucil, cisplatin, DN604 and **5** (15 μM) for 4 h. (**B**) Comet assay revealing increased chromosomal DNA strand breaks triggered by the measured compounds in A549 and A549/CDDP cells. (**C**) Compound **5** induced DNA damage in the nuclear genome and mitochondrial genome. (**D**) Intracellular DNA damage of the measured compounds. γH2AX foci after treatments was counted in 50-60 individual cells per time points of 12 h in A549 and A549/CDDP cells. Results are representative of at least three independent experiments and shown as the mean ± S.D. *P < 0.05, **P < 0.01 compared with control group.

Fig. 8. Compound **5** inhibited CK2-mediated MRN complex expression. (**A**) Inhibition of MRE11, RAD50 and NBS1 by the measured compounds. Western blot analyses of A549/CDDP cells after treatment with chlorambucil, cisplatin, DN604 and compound **5** for 24 h. (**B**) γH2AX foci kinetic repair following the treatment of cisplatin and compound **5**. A549/CDDP cancer cells were transfected with wild-type and siMRE11. Untransfected cancer cells were used as control. The γH2AX Foci were

JPET Fast Forward. Published on September 15, 2017 as DOI: 10.1124/jpet.117.243451
This article has not been copyedited and formatted. The final version may differ from this version.

counted in 50-60 individual cells per time point. (**C**) DSB repair kinetics after the treatment of measured compounds in wild-type and MRE11$^{-/-}$ cells. Untransfected cancer cells were used as control. The γH2AX Foci were counted in 50-60 individual cells per time point. (**D**) The effect of compound **5** on CK2 activity. (**E**) Transient overexpression of CK2 subunits increases CK2 activity. A549/CDDP cells were transfected with empty vector, Myc-His-tagged CK2α, and Myc-Histagged CK2β or co-transfected with Myc-His-tagged CK2α plus Myc-His-tagged CK2β. (**F**) Overexpression of CK2 subunits increased MRE11 protein expression. A549/CDDP cells were transiently co-transfected with the CK2 subunit plasmids. (**G**) Overexpression of CK2 subunits increased MRE11 protein expression induced by compound **5**. (**H**) Long-term colony formation assays of A549/CDDP cells. Cells were co-transfected with the CK2 subunit plasmids and grown in the presence of the measured compounds for 7 days. For each cell line, all dishes were fixed at the same time, stained and analyzed. (**I**) Co-transfection of CK2 subunits reduced the compound **5**-induced cell death. Results are representative of at least three independent experiments and shown as the mean ± S.D. **P* < 0.05, ***P* < 0.01 compared with control group. #*P* < 0.05, ##*P* < 0.01 compared with cancer cells transfected with empty vector.

Fig. 9. *In vivo* antitumor activity of cisplatin, chlorambucil, DN604 and **5** in

JPET Fast Forward. Published on September 15, 2017 as DOI: 10.1124/jpet.117.243451
This article has not been copyedited and formatted. The final version may differ from this version.

A549/CDDP xenograft tumors. (**A**) The tumor growth curve at the administration of the corresponding groups. Results are representative of at least three independent experiments and shown as the mean ± S.D. **P* < 0.05, ***P* < 0.01 compared with control group. (**B**) The tumor weight in each group at the end of the experiment. (**C**) Measured weight loss of mice during the treatments. Results are representative of at least three independent experiments and shown as the mean ± S.D. **P* < 0.05, ***P* < 0.01 compared with control group. (**D**) The HE staining of normal tissues of Liver and Kindey. (**E**) Tissues and tumor distribution of cisplatin and **5** in mice bearing A549/CDDP tumors after administration of the corresponding groups. Major organs were collected at 1 h after injection. (**F**) Stability of compound **5** in rat plasma. (**G**) *In vivo* pharmacokinetic curves of Pt concentration in the rat plasma versus time after intracenous injection of cisplatin and compound **5** in rats. Results are representative of at least three independent experiments and shown as the mean ± S.D. **P* < 0.05, ***P* < 0.01 compared with control group.

JPET Fast Forward. Published on September 15, 2017 as DOI: 10.1124/jpet.117.243451
This article has not been copyedited and formatted. The final version may differ from this version.

TABLE 1. *In Vitro* Cytotoxicity of Measured Samples

	IC_{50} (μM)[a]						
Compounds	SGC-7901	SGC-7901/CDDP	A549	A549/CDDP	HUVEC	RF1[b]	RF2[c]
Chlorambucil	80.25±10.75	101.64±18.76	75.85±10.13	120.98±19.76	165.95±29.46		
Cisplatin	1.73±0.11	12.26±0.93	2.06±0.15	19.75±0.96	10.35±3.72	7.09	9.59
Oxaliplatin	13.29±1.91	15.95±1.83	17.95±9.08	20.27±10.82	25.92±10.05		
Carboplatin	19.28±7.05	20.13±7.35	10.98±3.36	19.27±9.63	150.21±24.85		
DN603	12.84±3.78	16.59±7.53	10.32±8.91	20.39±10.12	30.72±13.42		
DN604	5.13±0.21	5.09±0.25	4.59±0.55	4.01±0.12	30.85±15.02	0.99	0.87
Compound **5**	3.59±0.32*	2.91±0.12**	3.38±0.16	1.95±0.92**	50.92±14.25**	0.81	0.58
Compound **6**	8.23±0.75**	15.28±7.56	8.05±0.92*	20.79±1.39	49.72±13.25**		

[a]IC_{50} is the drug concentration able to inhibit 50% of cell viability measured by MTT assay after 72 h drug exposure.

MTT = 3-(4,5-dimethylthiazol-2-yl)-2,5-diphenyltetrazolium bromide.

[b]Resistance Factor, IC_{50}(SGC-7901/CDDP)/IC_{50}(SGC-7901).

[c]Resistance Factor, IC_{50}(A549/CDDP)/IC_{50}(A549).

*$P < 0.05$, **$P < 0.01$ compared with cisplatin-treated group

JPET Fast Forward. Published on September 15, 2017 as DOI: 10.1124/jpet.117.243451
This article has not been copyedited and formatted. The final version may differ from this version.

Scheme 1. Synthesis of Pt(IV) compounds **5-6**[a].

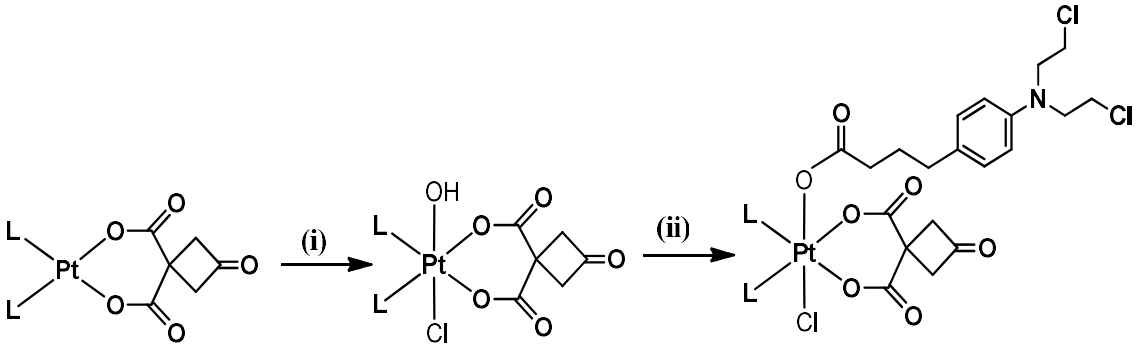

1- 2 **3 - 4** **5 - 6**

1, 3, 5: L = NH_3 ; 2, 4, 6: L, L = DACH; DACH = *1R,2R*-cyclohexanediamine

[a]Reaction conditions: (i) N-chlorosuccinimide(NCS), H_2O, room temperature, 3h in the dark; (ii) Chlorambucil, TBTU, TEA, DMF, 30 °C in the dark, 24h.

JPET Fast Forward. Published on September 15, 2017 as DOI: 10.1124/jpet.117.243451
This article has not been copyedited and formatted. The final version may differ from this version.

Fig. 1.

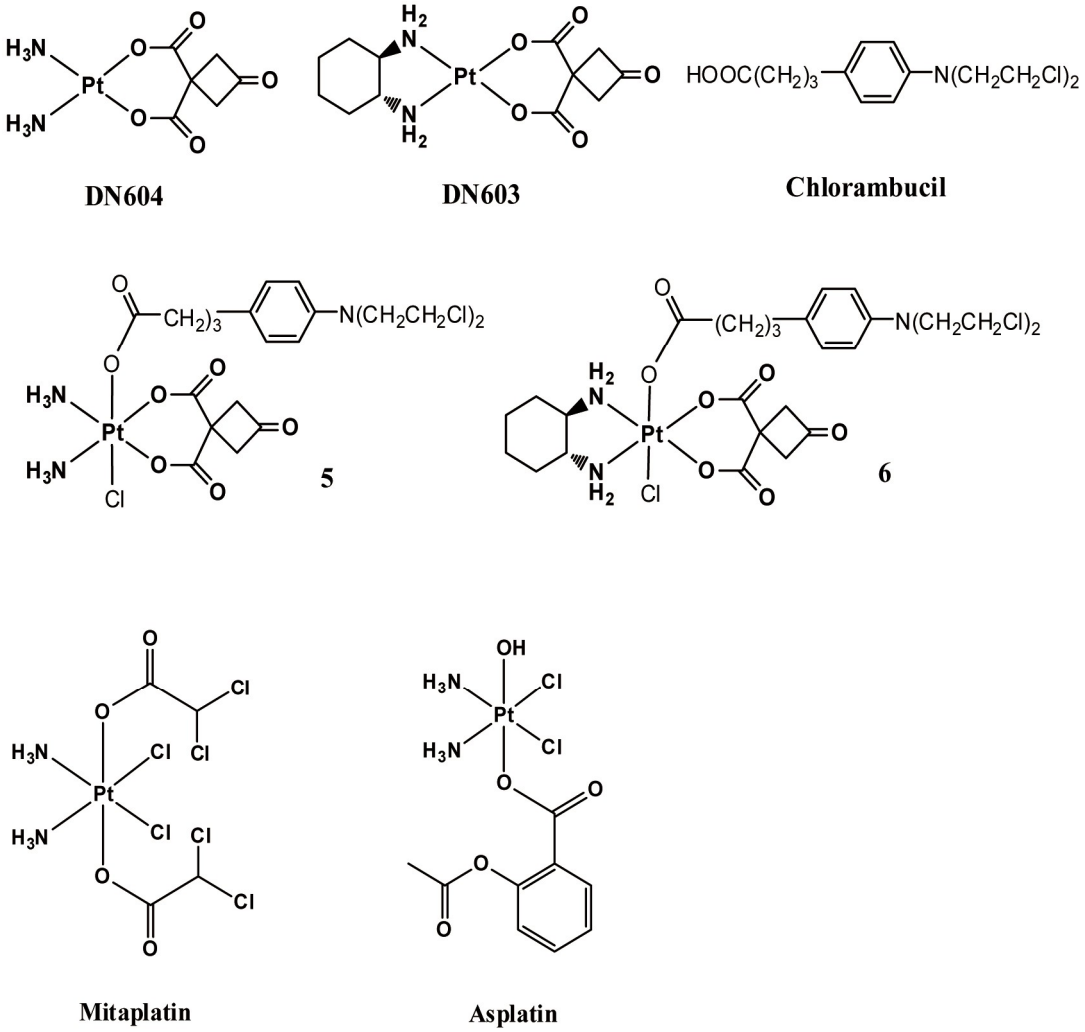

JPET Fast Forward. Published on September 15, 2017 as DOI: 10.1124/jpet.117.243451
This article has not been copyedited and formatted. The final version may differ from this version.

Fig. 2.

A

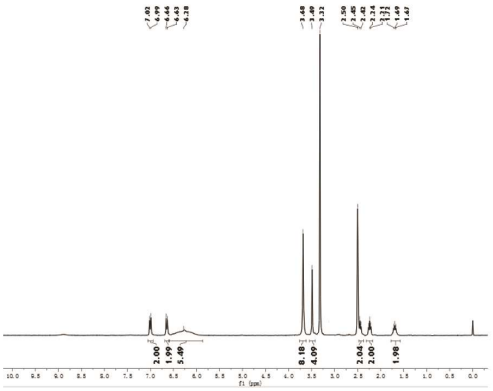

B

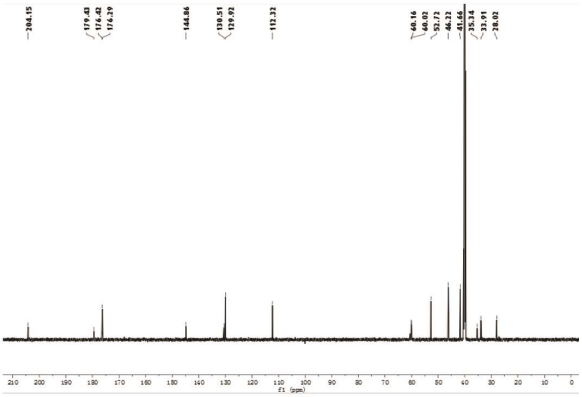

C

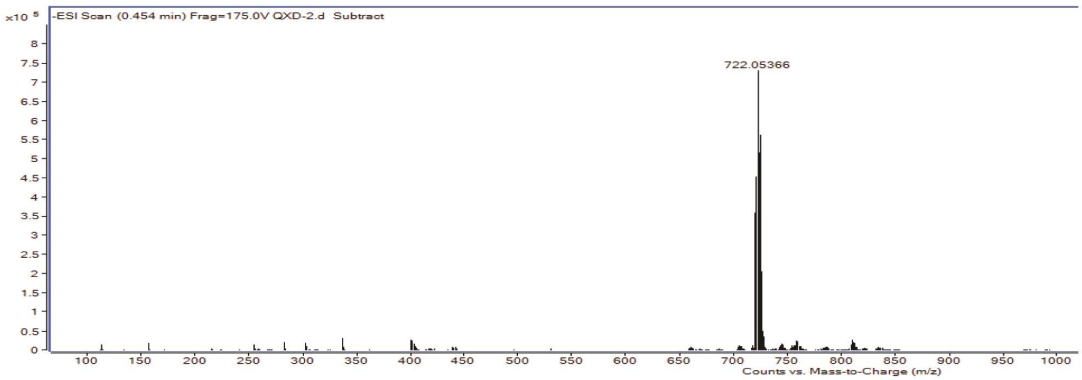

JPET Fast Forward. Published on September 15, 2017 as DOI: 10.1124/jpet.117.243451
This article has not been copyedited and formatted. The final version may differ from this version.

Fig. 3.

A

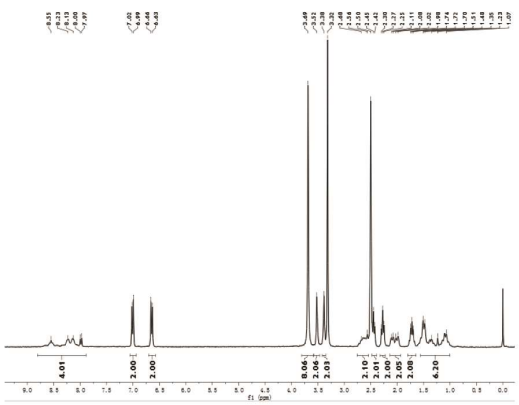

B

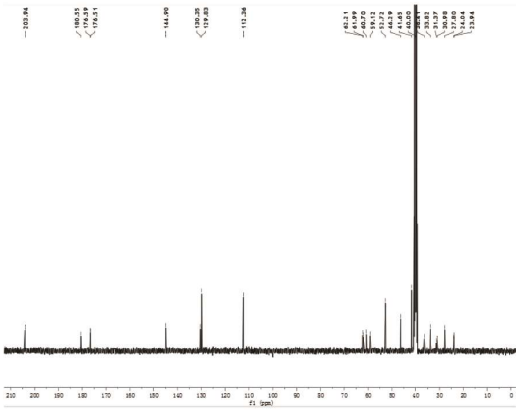

C

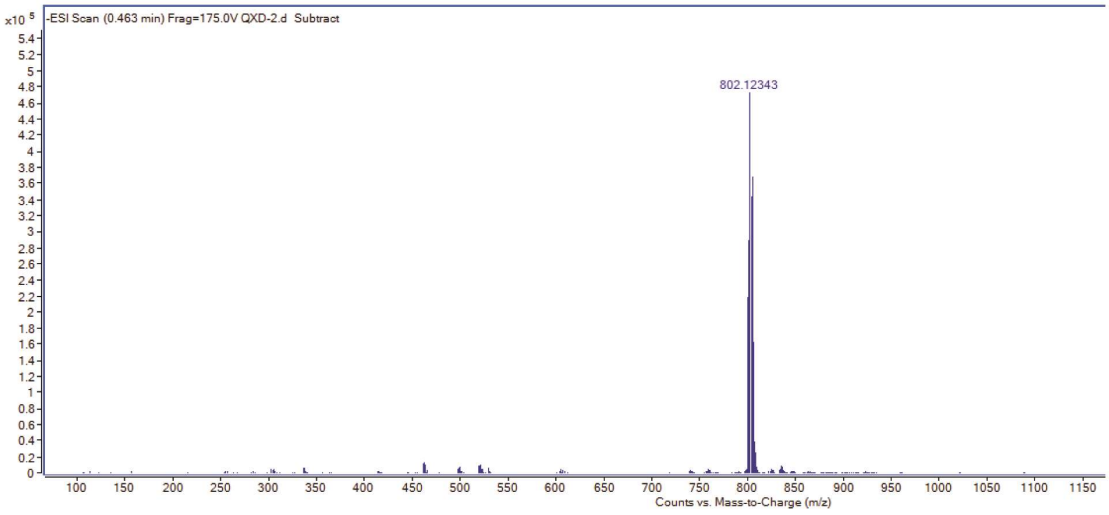

JPET Fast Forward. Published on September 15, 2017 as DOI: 10.1124/jpet.117.243451
This article has not been copyedited and formatted. The final version may differ from this version.

A

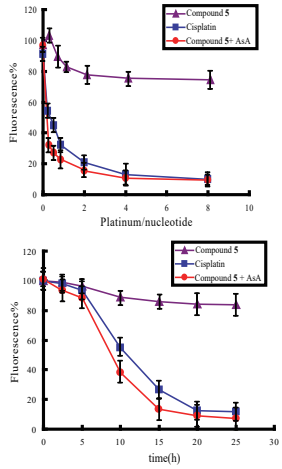

B

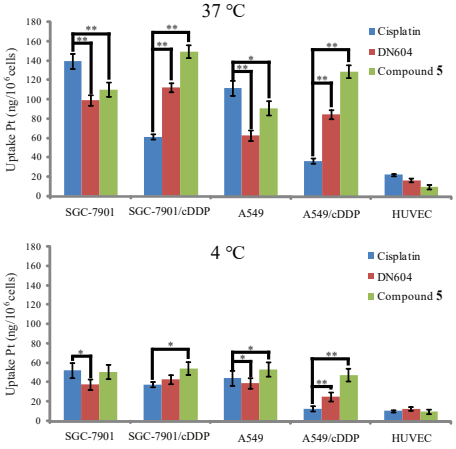

Compounds	Pt content (ng/10^6 cells)				
	SGC-7901	SGC-7901/cDDP	A549	A549/cDDP	HUVEC
Cisplatin	139±21.2	59±7.4	118±20.9	39±7.3	26±5.8
DN604	98±8.9	115±15.8	60±12.7	86±9.2	18±3.6
Compound **5**	109±10.8	149±11.3	96±19.5	129±21.9	10±2.7

Compounds	Pt content (ng/10^6 cells)				
	SGC-7901	SGC-7901/cDDP	A549	A549/cDDP	HUVEC
Cisplatin	49±3.6	32±2.1	44±2.9	15±2.3	12±1.8
DN604	38±4.9	41±6.8	42±3.7	24±5.2	13±1.6
Compound **5**	48±5.8	51±6.3	53±9.5	43±8.5	8±0.7

C

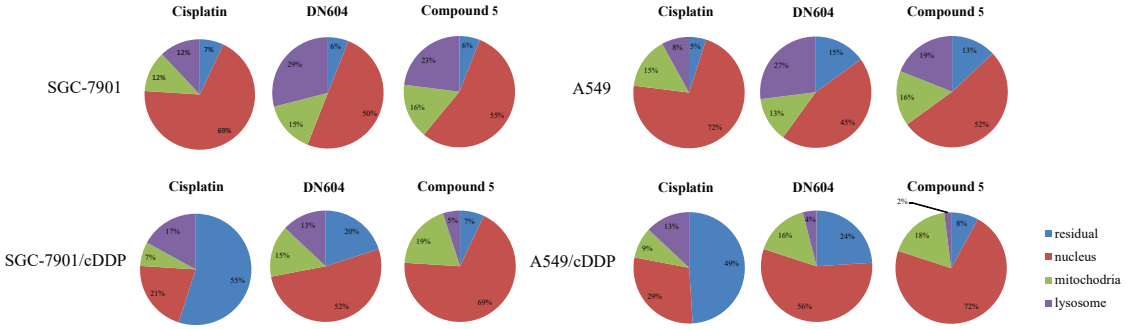

D

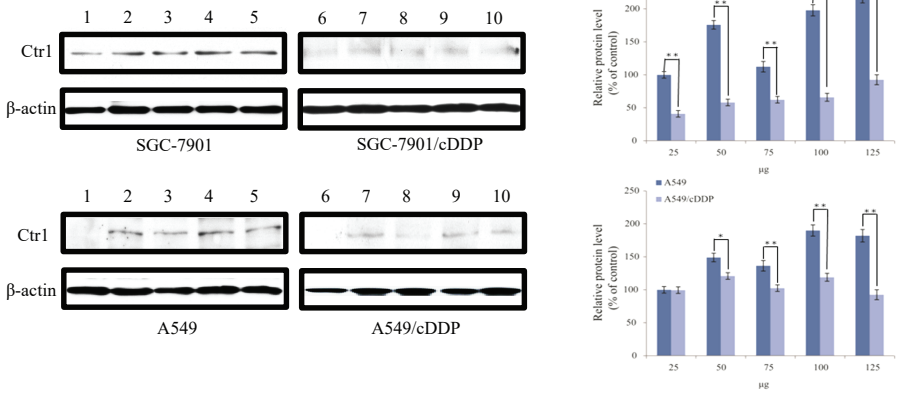

E

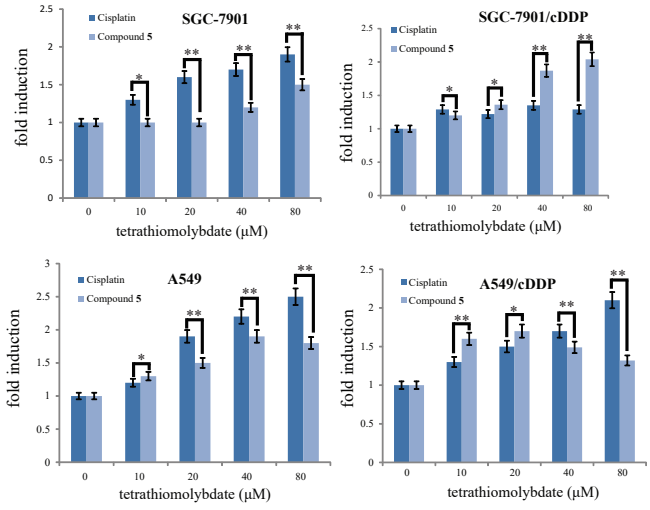

JPET Fast Forward. Published on September 15, 2017 as DOI: 10.1124/jpet.117.243451
This article has not been copyedited and formatted. The final version may differ from this version.

Fig. 5.

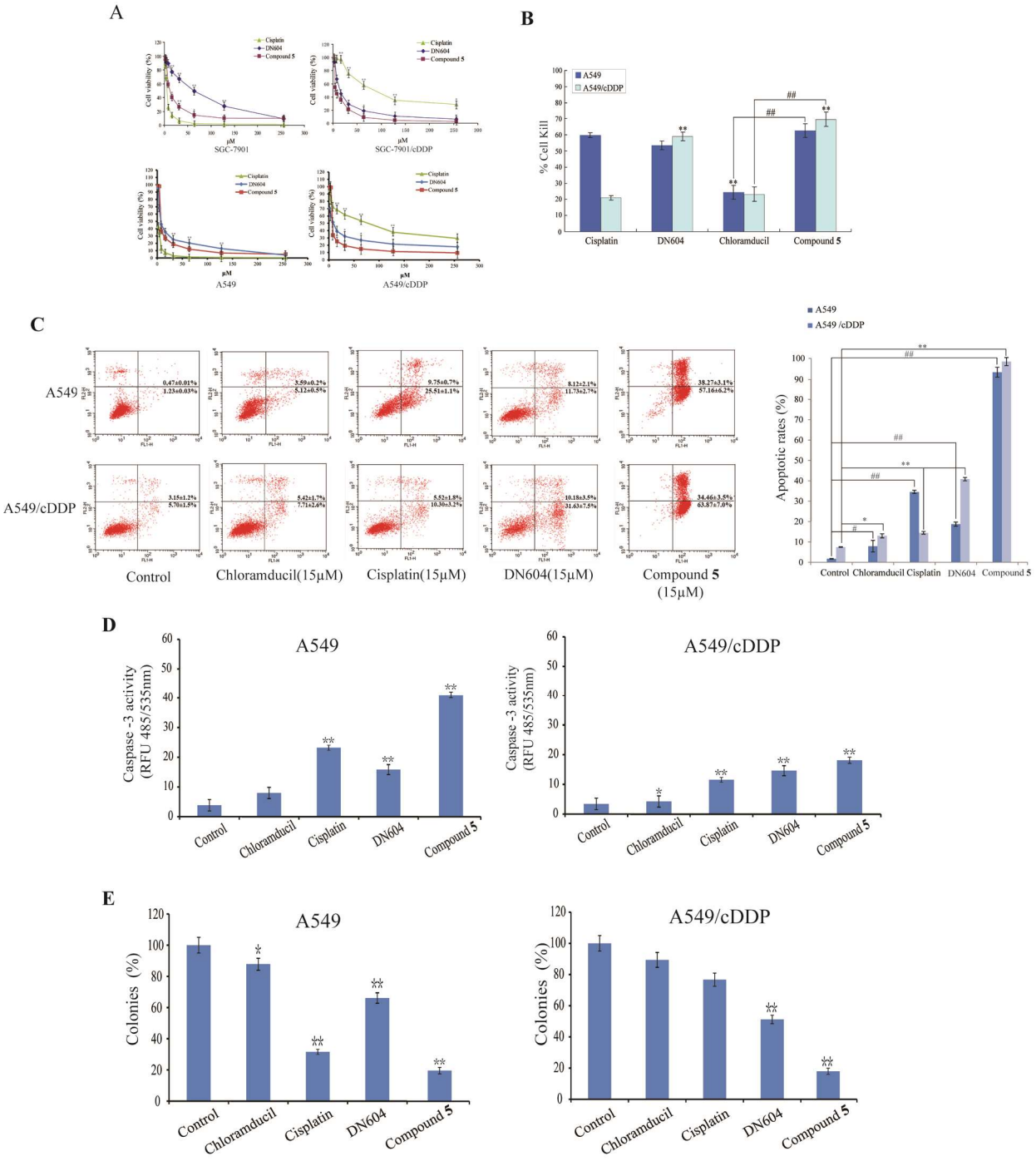

JPET Fast Forward. Published on September 15, 2017 as DOI: 10.1124/jpet.117.243451
This article has not been copyedited and formatted. The final version may differ from this version.

Fig. 6.

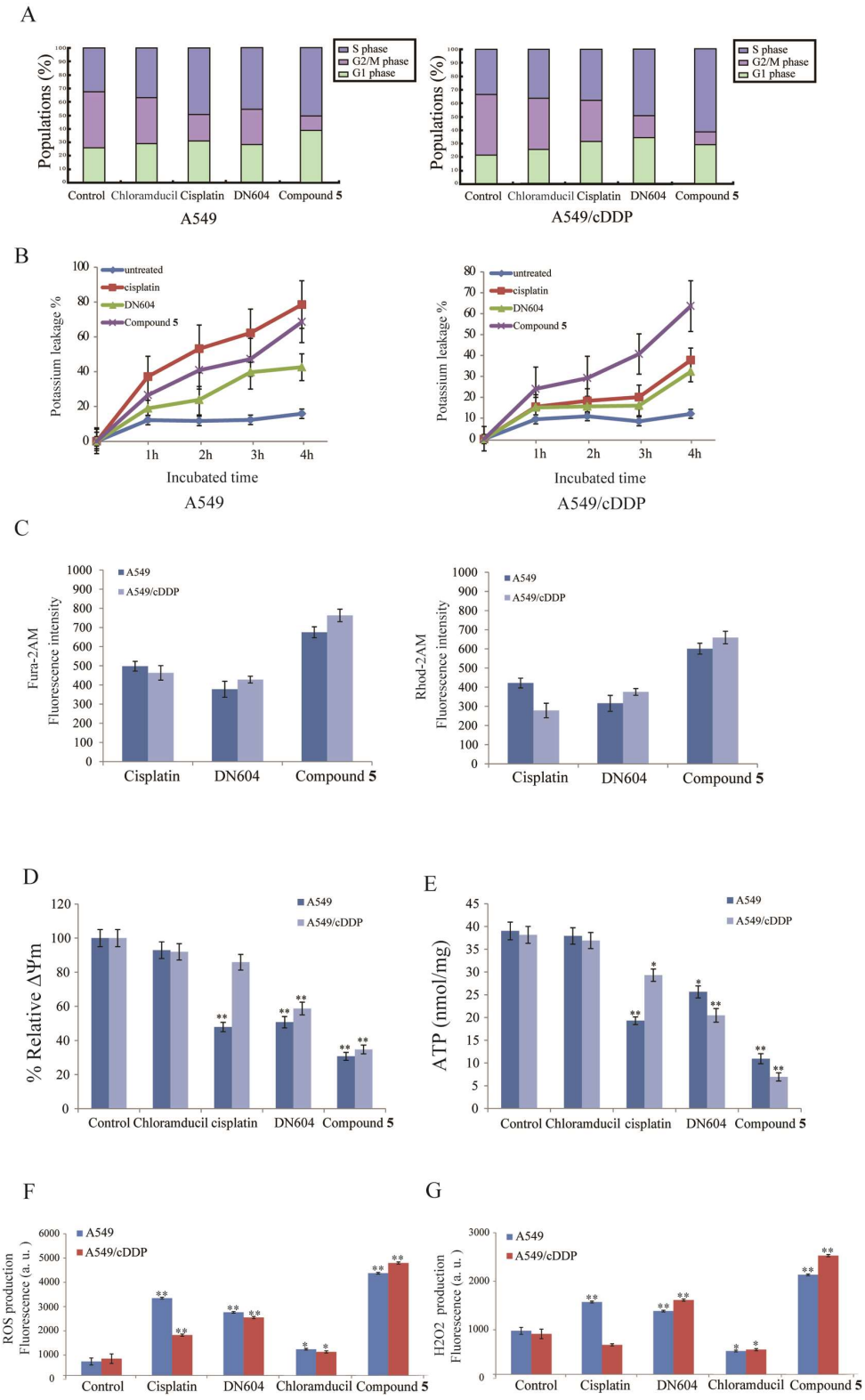

JPET Fast Forward. Published on September 15, 2017 as DOI: 10.1124/jpet.117.243451
This article has not been copyedited and formatted. The final version may differ from this version.

Fig. 7.

A

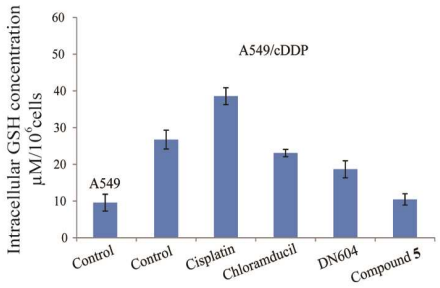

B

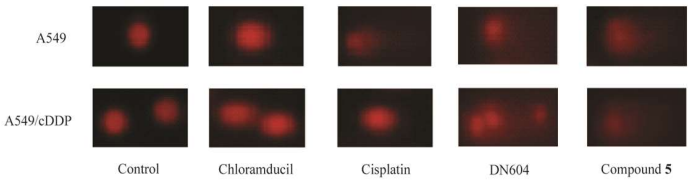

semiquantitative results of comet assay (A549 and A549/cDDP)

	Control	Chloramducil	Cisplatin	DN604	Compound **5**
Tail Length	6.59±1.35/7.02±1.01	12.94±2.24/22.47±3.21	39.73±13.15/26.87±11.92	27.96±12.19/17.82±9.75	57.93±19.72/39.84±15.62
Tail Moment	1/27±1.12/1.32±0.64	0.95±0.06/2.15±0.91	8.43±0.68/5.16±0.41	8.82±0.12/3.47±0.95	19.28±9.21/6.04±1.29
Oliva Tail Moment	0.57±0.07/0.49±0.08	2.59±0.32/1.62±0.95	3.19±1.36/2.48±1.05	2.41±0.81/1.37±0.91	7.38±2.04/6.71±0.94

C

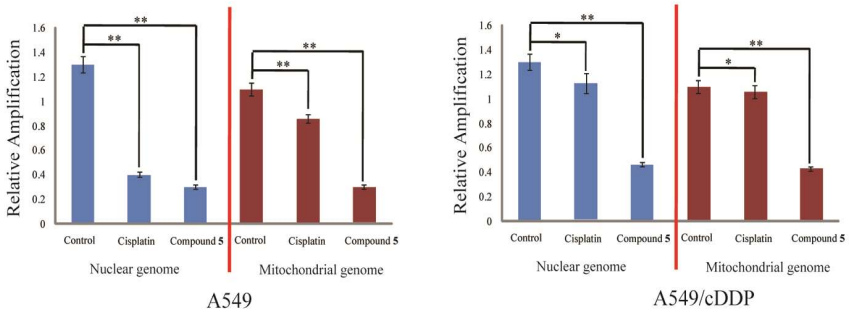

D

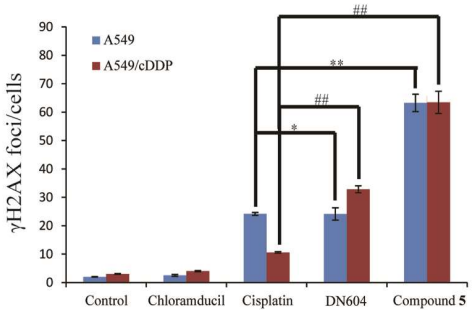

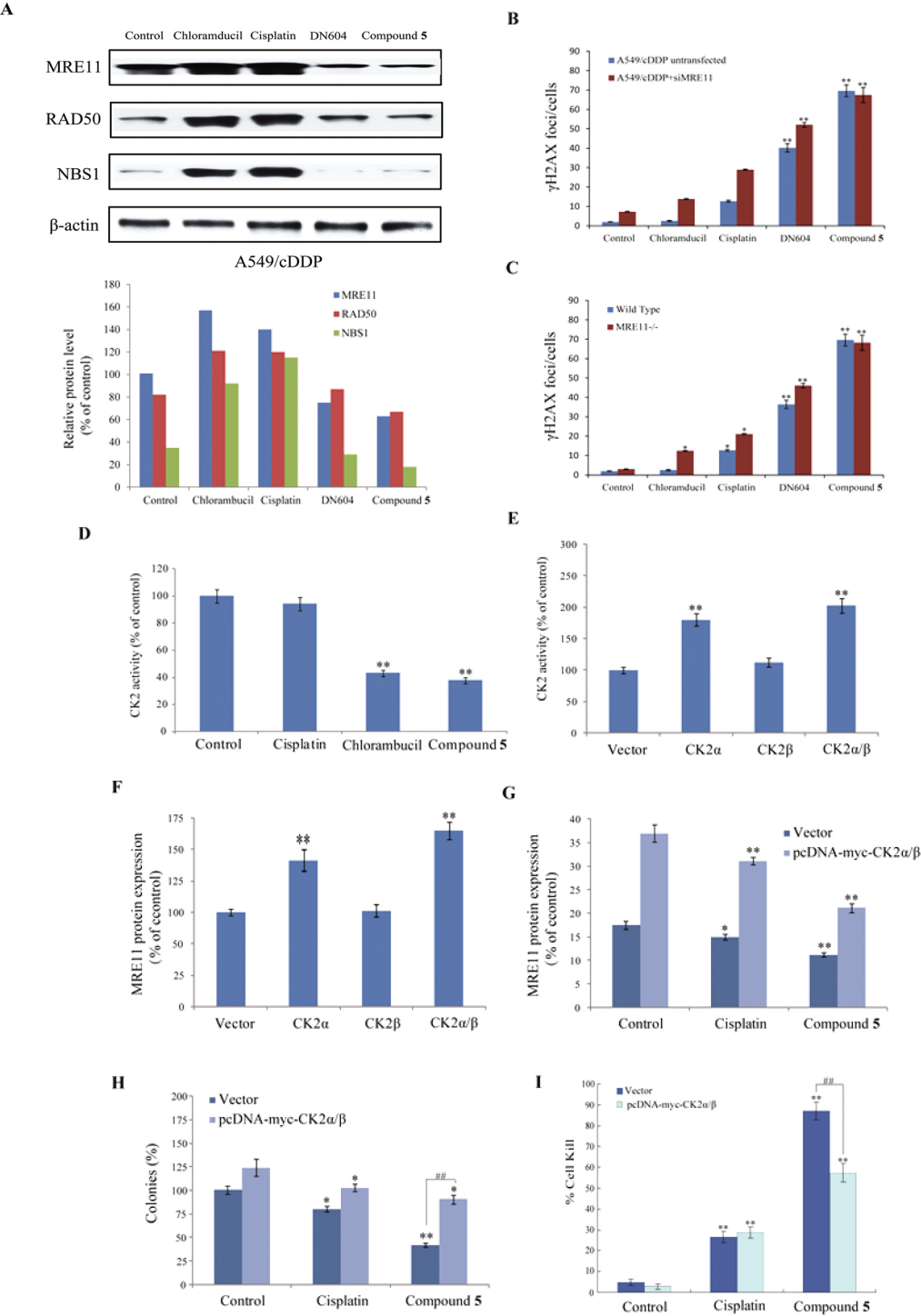
A
Control
Chloramducil
Cisplatin
DN604
Compound 5
MRE11
RAD50
NBS1
β-actin
A549/cDDP
Relative protein level (% of control)
MRE11
RAD50
NBS1
Control
Chlorambucil
Cisplatin
DN604
Compound 5
B
A549/cDDP untransfected
A549/cDDP+siMRE11
γH2AX foci/cells
Control
Chloramducil
Cisplatin
DN604
Compound 5
C
Wild Type
MRE11-/-
γH2AX foci/cells
Control
Chloramducil
Cisplatin
DN604
Compound 5
D
CK2 activity (% of control)
Control
Cisplatin
Chlorambucil
Compound 5
E
CK2 activity (% of control)
Vector
CK2α
CK2β
CK2α/β
F
MRE11 protein expression (% of control)
Vector
CK2α
CK2β
CK2α/β
G
Vector
pcDNA-myc-CK2α/β
MRE11 protein expression (% of control)
Control
Cisplatin
Compound 5
H
Vector
pcDNA-myc-CK2α/β
Colonies (%)
Control
Cisplatin
Compound 5
I
Vector
pcDNA-myc-CK2α/β
% Cell Kill
Control
Cisplatin
Compound 5

JPET Fast Forward. Published on September 15, 2017 as DOI: 10.1124/jpet.117.243451
This article has not been copyedited and formatted. The final version may differ from this version.

Fig. 9.